2018-04-01

Large-Scale Strength Testing of High-Speed Railway Bridge Embankments: Effects of Cement Treatment and Skew Under Passive Loading

Daniel Ethan Schwicht
Brigham Young University

Large-Scale Strength Testing of High-Speed Railway Bridge Embankments:

Effects of Cement Treatment and Skew Under Passive Loading

Daniel Ethan William Schwicht

A thesis submitted to the faculty of
Brigham Young University
in partial fulfillment of the requirements for the degree of

Master of Science

Kyle M. Rollins, Chair
Kevin W. Franke
Norman L. Jones

Department of Civil and Environmental Engineering

Brigham Young University

ABSTRACT

Large-Scale Strength Testing of High-Speed Railway Bridge Embankments:
Effects of Cement Treatment and Skew Under Various Loading

Daniel Ethan William Schwicht
Department of Civil and Environmental Engineering, BYU
Master of Science

To investigate the passive force-displacement relationships provided by a transitional zoned backfill consisting of cement treated aggregate (CTA) and compacted gravel, a series of full-scale lateral abutment load tests were performed. The transitional zoned backfill was designed to minimize differential settlement adjacent to bridge abutments for the California High Speed Rail project. Tests were performed with a 2-D or plane strain backfill geometry to simulate a wide abutment. To investigate the effect of skew angle on the passive force, lateral abutment load tests were also performed with a simulated abutment with skew angles of 30º and 45º.

The peak passive force developed was about 2.5 times higher than that predicted with the California HSR design method for granular backfill material with a comparable backwall height and width. The displacement required to develop the peak passive force decreased with skew angle and was somewhat less than for conventional granular backfills. Peak passive force developed with displacements of 3 to 1.8% of the wall height, H in comparison to 3 to 5% of H for conventional granular backfills.

The skew angle had less effect on the peak passive force for the transitional backfill than for conventional granular backfills. For example, the passive force reduction factor, R_{skew}, was only 0.83 and 0.51 for the 30º and 45º skew abutments in comparison to 0.51 and 0.37 for conventional granular backfills. Field measurements suggest that the CTA backfill largely moves with the abutment and does not experience significant heave while shear failure and heaving largely occurs in the granular backfill behind the CTA backfill zone.

Keywords: bridge abutment, bridge embankment, cement treatment, full-scale testing, high-speed rail, passive strength, plate-load test, skew, skew reduction factor, transitional zone

ACKNOWLEDGEMENTS

I am grateful for my wife, who is unfailingly understanding, supportive, and practical, through days of physical labor, hours of high-pitched complaining, evenings of overwhelmed frustration, and nights of data wrestling. Without her, I would have given up before I ever started, and I certainly never could have finished.

Dr. Kyle Rollins is one of the most brilliant and kindest people I have ever met. It is a privilege to work with him. He has consistently treated me as a respected peer—an enormous overestimation of my capacity and a vote of confidence that has deeply affected me as an engineer and as a person.

Dave Anderson and Rodney Mayo worked countless hours to bring about the experiments recorded in these pages. Without their flexibility and patience with a tumultuous schedule, the project would have died on the vine several times over. Moreover, working alongside them made long days seem manageable.

Rebecca Black's unhesitating willingness to help however she was needed was critical to every facet of this research. Her friendship was critical to my maintaining a good attitude.

I also express gratitude to Anoosh Shamsabadi, WSP, and California High Speed Rail Authority for the funding which allowed our research to take place.

TABLE OF CONTENTS

LIST OF FIGURES

LIST OF TABLES

1 INTRODUCTION

To understand the topics discussed, a brief introduction is necessary. This section discusses the context and purposes of this thesis, including a brief look at existing research on high-speed railway settlement issues at abutment-embankment transition zones and the effect of abutment skew angle on embankment passive resistance. The research objectives of this thesis and scope of work are defined.

1.1 Background

High-speed rail track experiences accelerated degradation or differential settlement in zones of transition, such as at bridge abutments. This degradation is due to a difference in stiffness between the bridge (often pile-supported) and the approach or departure (often compacted sand or gravel) (Paixão et al. 2013). Each railroad company in the United States spends an estimated $25.5 million yearly on repairs for these transition zones (Nicks 2009). In order to reduce the differential settlement in these transition zones, California High Speed Rail (HSR) has designed a bridge abutment with a transition zone consisting of cement treated aggregate (CTA) as a stiffness transition from the bridge to compacted gravel. Although passive force-deflection relationships are well defined for conventional compacted backfill materials (Rollins and Cole 2006; Shamsabadi et al. 2007), no test results are available to define the passive force-deflection behavior for transition zones with CTA between the bridge abutment and the compacted gravel backfill.

In addition, many of the bridge abutments for California High Speed Rail will be skewed relative to the underlying roadways. Abutment skew angle (θ), as shown in

Figure 1-1, is the angle of the back wall of the abutment relative to a line perpendicular to the direction of travel.

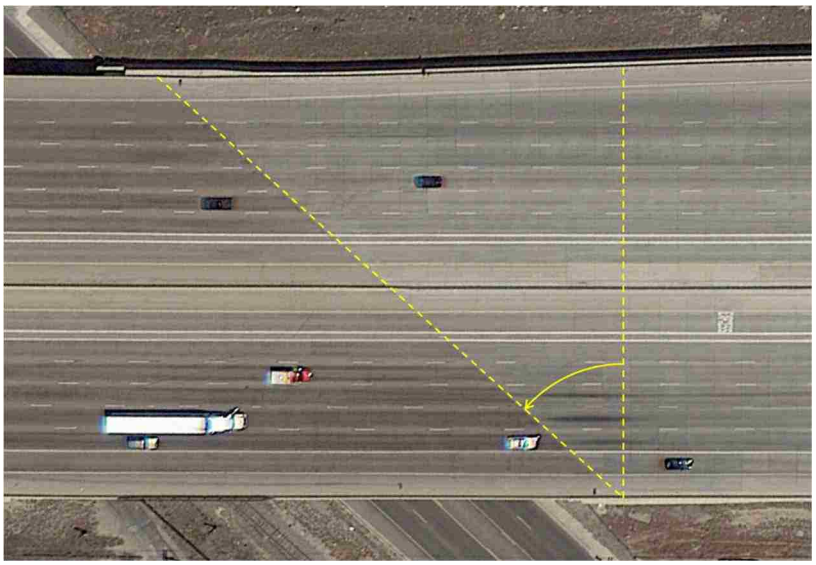

Figure 1-1. Skewed bridge abutment.

A large number of small- and large-scale tests have shown that skewed abutments develop lower passive resistance than non-skewed abutments (Rollins and Jessee 2013; Marsh 2013; Franke 2013; Palmer 2013; Smith 2014; Frederickson et al. 2017) with backfills consisting of sands or gravels. A skew reduction factor (R_{skew}) can account for reduced passive resistance as a function of skew angle (Rollins and Jessee 2013). Based on all available testing, R_{skew} is defined with the equation

$$R_{skew} = \frac{P_{p-skew}}{P_{p-no\ skew}} = e^{\left(\frac{-\theta}{45^{\circ}}\right)} \quad (1)$$

for backfills composed of sand or gravel (Shamsabadi and Rollins 2014). Equation 1 predicts a reduction in passive force of about 50% for a 30º skew angle. Transitional backfills with CTA

and gravel zones have never been tested for skew angle passive capacity reduction; however, small-scale abutment tests with low strength flowable fill backfills (unconfined compressive strength of about 60 psi or 410 kPa) showed little to no reduction in passive force with skew angle (Wagstaff, 2015). As a result, there is considerable uncertainty about the influence of skew angle on passive resistance for the transitional backfills proposed for California High Speed Rail. To investigate the effect of transitional zones with CTA backfill on passive force-deflection relationships and the effect of skew angle, a series of full-scale passive force tests were conducted in this study.

1.2 Research Objectives

The research objectives for this study are:

1. Determine passive force-displacement relationships for CTA transitional backfills from full-scale tests
2. Quantify the effect of skew angle on the passive force for CTA transitional backfills

1.3 Scope of Work

Passive force-deflection relationships were measured for a series of full-scale simulated bridge abutment tests with skew angles of 0˚, 30˚, and 45˚. Backfill geometry consisted of a zone of CTA backfill behind the abutment wall with a zone of compacted gravel behind the CTA backfill in general agreement with the typical design section proposed by California High Speed Rail. Lab testing was performed to characterize the material properties of the aggregate and CTA. For each test configuration, quality control testing was performed during backfill placement. These full-scale passive load tests were performed at the Brigham Young University (BYU) test site located at the Salt Lake International Airport.

2 TEST DESIGN

The California HSR design, shown in Figure 2-1, specified backfill material characteristics, installation density standards, and abutment and embankment geometry.

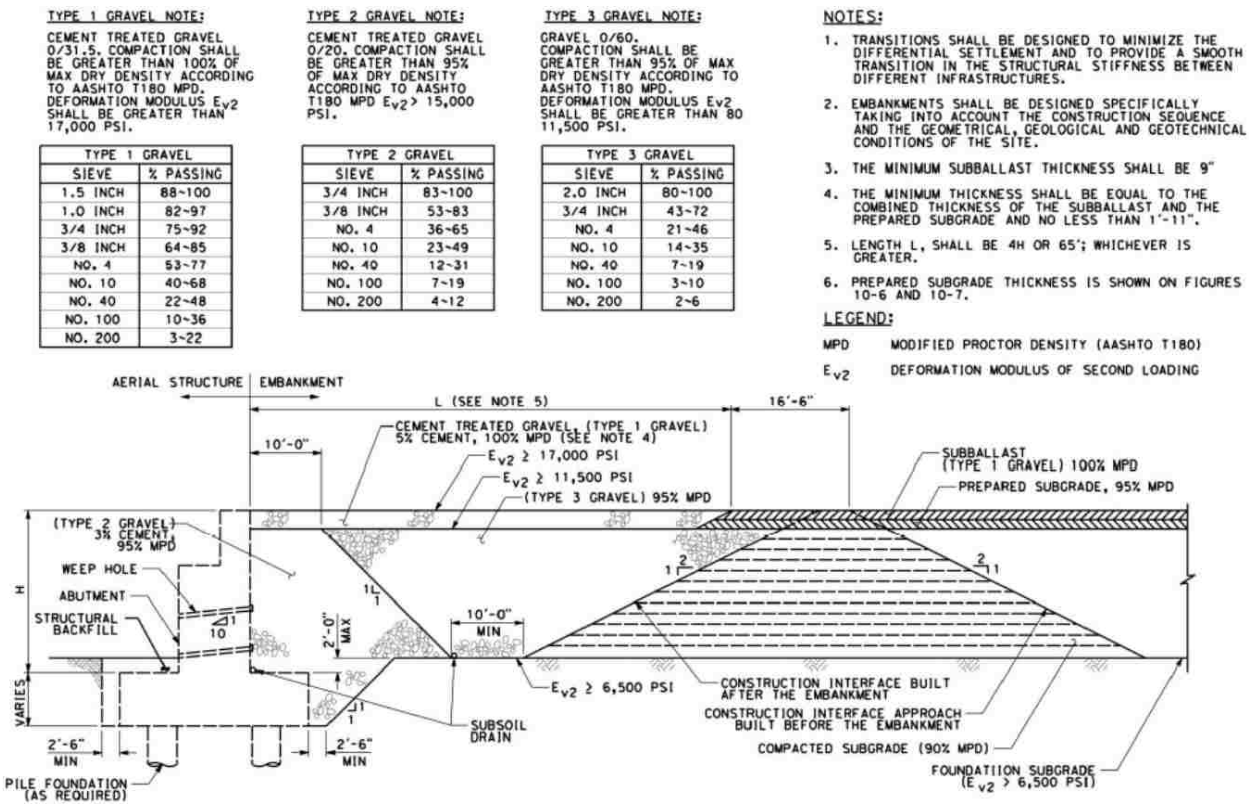

Figure 2-1. California HSR transition from bridge, aerial structure, or grade separation to embankment.

2.1 Material Characterization of Backfill

Investigations for full-scale tests included preliminary material characterization of both the CTA backfill (Type 2 Gravel with 3% cement) and granular backfill (Type 3 Gravel) as defined in Figure 2-1. Initially, particle-size analyses were performed (ASTM D6913/D6913M)

and moisture-density relationships were established (ASTM D1557). Relative compaction of both backfill zones was tested during placement using nuclear density testing. In addition, specimens of CTA were compacted into cylinders in the field for subsequent unconfined compressive strength (UCS) testing. Backfill materials were also tested for water-soluble sulfate concentration (ASTM C1580). Finally, plate load testing (DIN 18134) was performed on the surface of the CTA backfill zone after completion of the passive force testing.

2.2 Model Design and Quality Control

Plan and profile drawings are provided in Figure 2-2, Figure 2-3, and Figure 2-4 for the 0˚, 30˚, and 45˚ skew configurations, respectively. A pile cap 11 ft. wide by 5.5 ft. high by 15 ft. long (3.4 by 1.7 by 4.6 m) was used to simulate a bridge abutment. North of the pile cap, a trench or box of 11 ft. width by 6 ft. high by 32 ft. long (3.4 by 1.8 by 9.8 m) was backfilled to simulate the designed embankment. The embankment was composed of two zones, one zone of CTA and one of gravel. The transitional zone of CTA was placed and compacted against the pile cap and extending 10 ft. (3.0 m) from the pile cap at the embankment surface, then sloping downward with a 1H to 1V slope away from the pile cap. North of the CTA, a zone of Type 3 gravel was placed with a base width of 10 ft. (3.0 m), compacted against a 1H to 1V slope of gravel already in place.

The existing test site conditions required minor alterations to the geometry of the California HSR design, such as a simplification of the abutment-embankment interface to a flat wall and the deletion of the uppermost layer of cement treated Type 1 gravel. These alternations are not expected to materially affect the measured passive force or skew reduction factors determined from the testing.

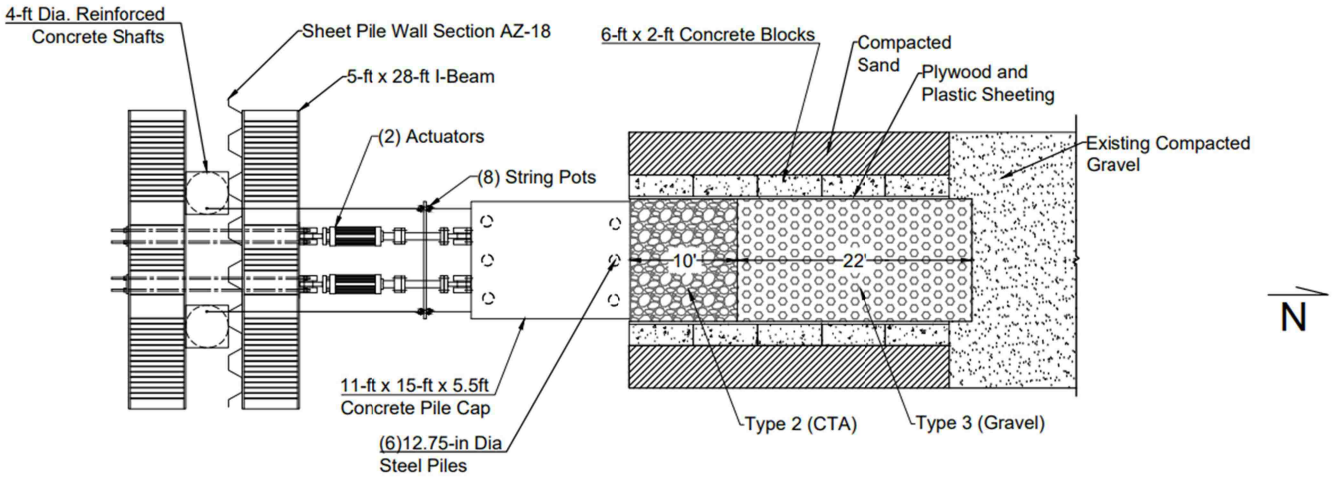

Figure 2-2. Schematic plan and elevation drawings of 0° skew test configuration.

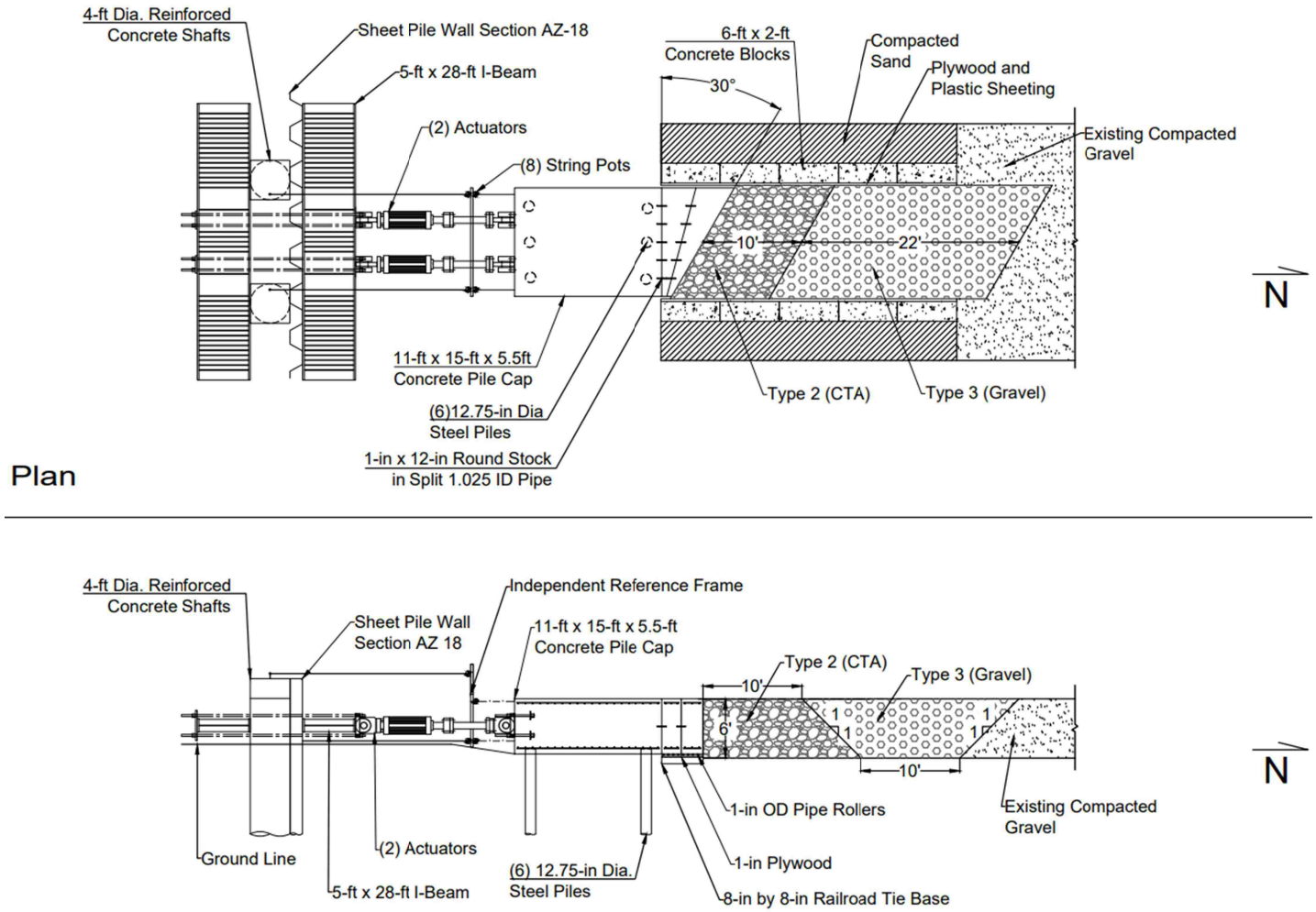

Figure 2-3. Schematic plan and elevation drawing of 30° skew test configuration.

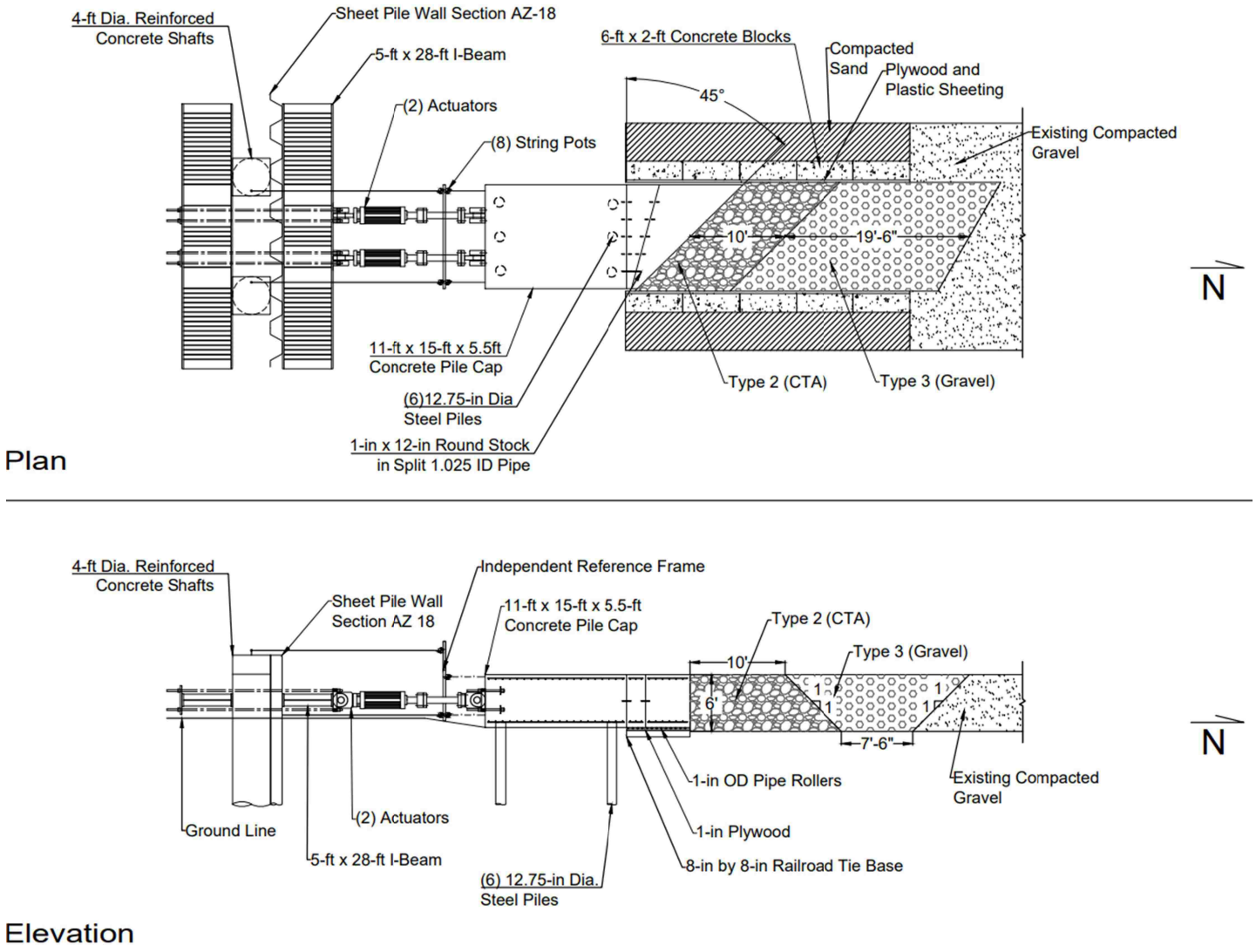

Figure 2-4. Schematic plan and elevation drawing of 45° skew test configuration.

To create a two-dimensional or plane strain failure geometry typical of a wide approach fill, plywood and a lubricated double layer of plastic sheeting lined the concrete block sidewalls on the east and west of the backfill zone to minimize side friction. Reinforced concrete skew wedge blocks were placed on wooden platforms with steel pipe rollers to decrease friction on the base of the skew wedges. For quality control, density and moisture testing was done using a nuclear density gauge to ensure compliance with the specified relative compaction of 95% of maximum dry density.

2.3 Passive Force Testing

Two 600 kip (2.7 MN) actuators were installed to push the pile cap until passive failure of the backfill. In order to measure the overall movement of the pile cap, string potentiometers (string pots) were installed on the upper and lower corners of the pile cap opposite the backfill, attached to an independent reference frame. Before installation of the backfill embankment, the actuators were used to find a baseline force-deflection curve for the pile cap and testing apparatus. Analysis was carried out to facilitate future embankment design.

2.4 Surface Displacement

After installation of backfill and before passive failure testing, a 2 ft. (0.6 m) grid was spray-painted on the surface of the backfill. Elevation data were collected before and after each test at each grid intersection using a digital level. A total station was used for analysis of horizontal deformation of embankment surface. String potentiometers were also installed at 2 ft. (0.6 m) intervals along the backfill surface to gather data on the deflection along the surface relative to the pile cap.

3 RESULTS AND ANALYSIS

This chapter contains the results of material characterization, the process of installation, the results and analysis of passive force testing, and the analysis of surface displacement.

3.1 Material Characterization of Backfill

Preliminary to backfilling, material characterization was performed to select suitable backfill materials. This testing included particle-size analysis, moisture-density relationship testing, and water-soluble sulfate concentration testing. After passive force testing, plate load testing was performed and CTA cylinders, cast during installation, were tested for their unconfined compressive strength (UCS).

3.1.1 Particle-Size Analysis

Backfill materials were tested for compliance with the California HSR specifications for particle-size distribution. Type 2 and Type 3 gravel backfills were needed for the transition zone. Figure 3-1 presents the particle-size distribution of the material selected for the Type 2 (CTA) backfill plotted in a solid green line with the upper and lower bound ranges for acceptable particle-size distribution plotted with dashed lines. Figure 3-2 provides a similar plot for the specially blended material used as Type 3 (gravel) backfill and the corresponding specified range plotted with dashed lines. In both cases, the backfill gradations fall within the specified boundaries.

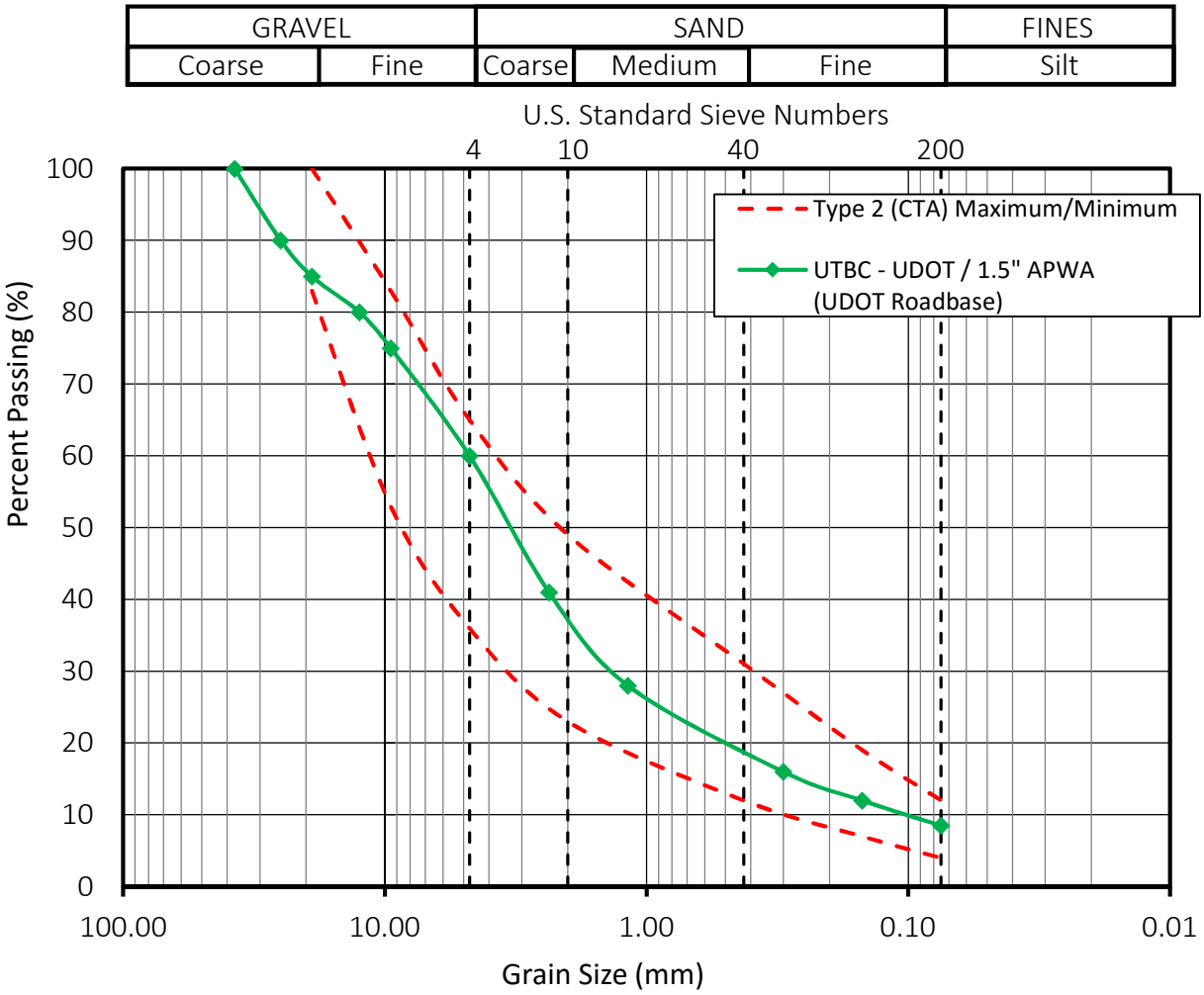

Figure 3-1. Type 2 specification and selected material particle-size analysis.

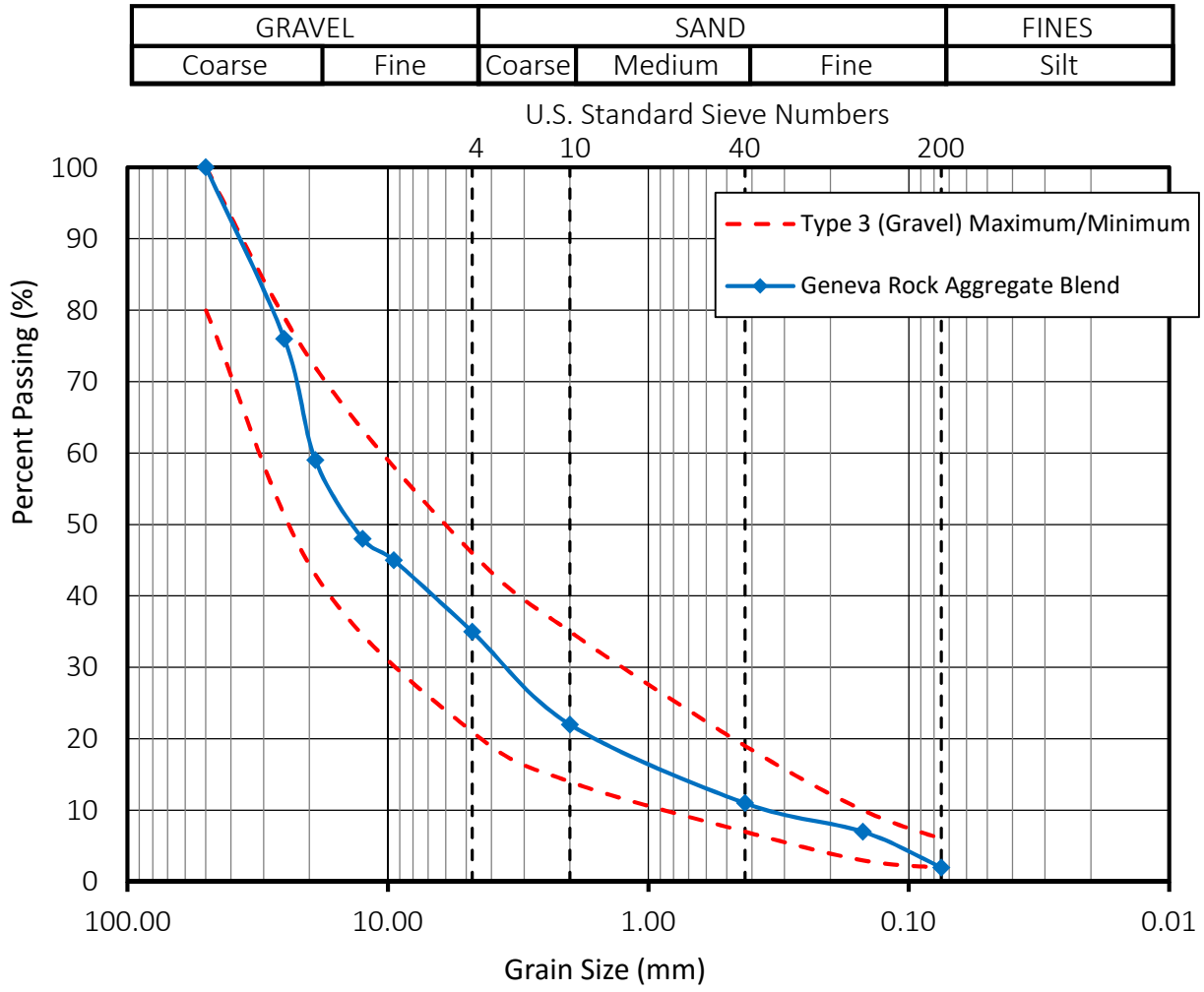

Figure 3-2. Type 3 specification and selected material particle-size analysis.

3.1.2 Moisture-Density Relationship

For both backfill material types, tests were performed to determine the modified Proctor moisture-density relationship (ASTM D1557). Testing on the CTA was performed at the specified cement content of 3% by mass. The maximum dry density for the Type 2 (CTA) backfill was 138 lbs/ft^3 (21.7 kN/m^3) with an optimum moisture content of 6.5%, while the maximum dry density for the Type 3 (gravel) was 135 lbs/ft^3 (21.2 kN/m^3) with an optimum moisture content of 6.5%.

3.1.3 Water-Soluble Sulfate Concentration in Soil

Water-soluble sulfates in soil used for concrete or CTA pose the risk of problematic chemical reactions. Delayed Ettringite formation can lead to severe expansion of CTA when sulfate concentrations exceed 3000 ppm (Portland Cement Association 1992). Testing was performed on the material selected for use as Type 3 (CTA) backfill to determine the water-soluble sulfate concentration (ASTM 1580), and the concentration was only 5.2 ppm, well below the 3000 ppm threshold.

3.1.4 Plate Loading Test

After completion of the 45˚ skew passive failure test, a plate load test was performed on the surface of the CTA zone in general accordance with DIN 18134. Figure 3-3 shows the testing setup.

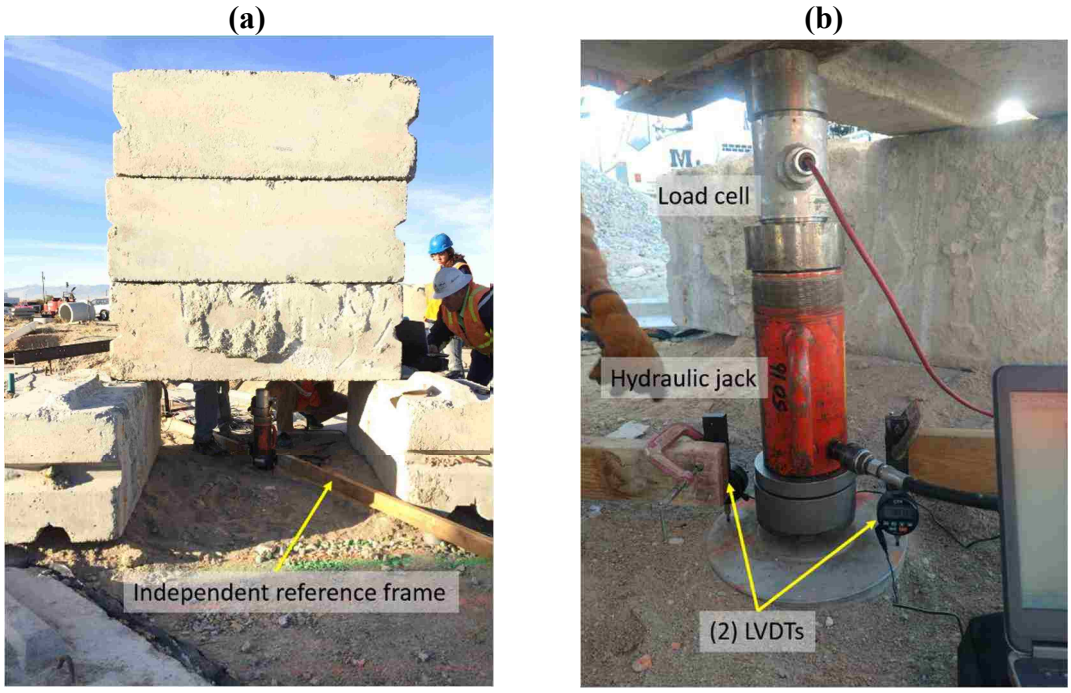

Figure 3-3. Plate load test setup showing (a) reference frame and reaction load, and (b) hydraulic jack, load cell, and LVDTs.

Three pre-cast concrete blocks (combined weight of 10,500 lb. (46.7 kN) was positioned above the plate to allow for the necessary maximum stress of 73 psi (0.5 MN/m^2). An independent reference frame was anchored outside of the area influenced by the loading as recommended. A load cell reported the load exerted by the hydraulic jack while linear variable differential transformers (LVDTs) were placed on opposing edges of the plate to record settlement. The resulting settlement versus normal stress is plotted below in Figure 3-4. E_{v2} is the strain modulus for the second loading cycle, calculated following DIN 18134. Using the coefficients from quadratic best fit lines, the E_{v2} calculated for the CTA is 1,270,000 psi (8780 MPa), which meets California HSR specifications of E_{v2} greater than 15,000 psi (100 MPa).

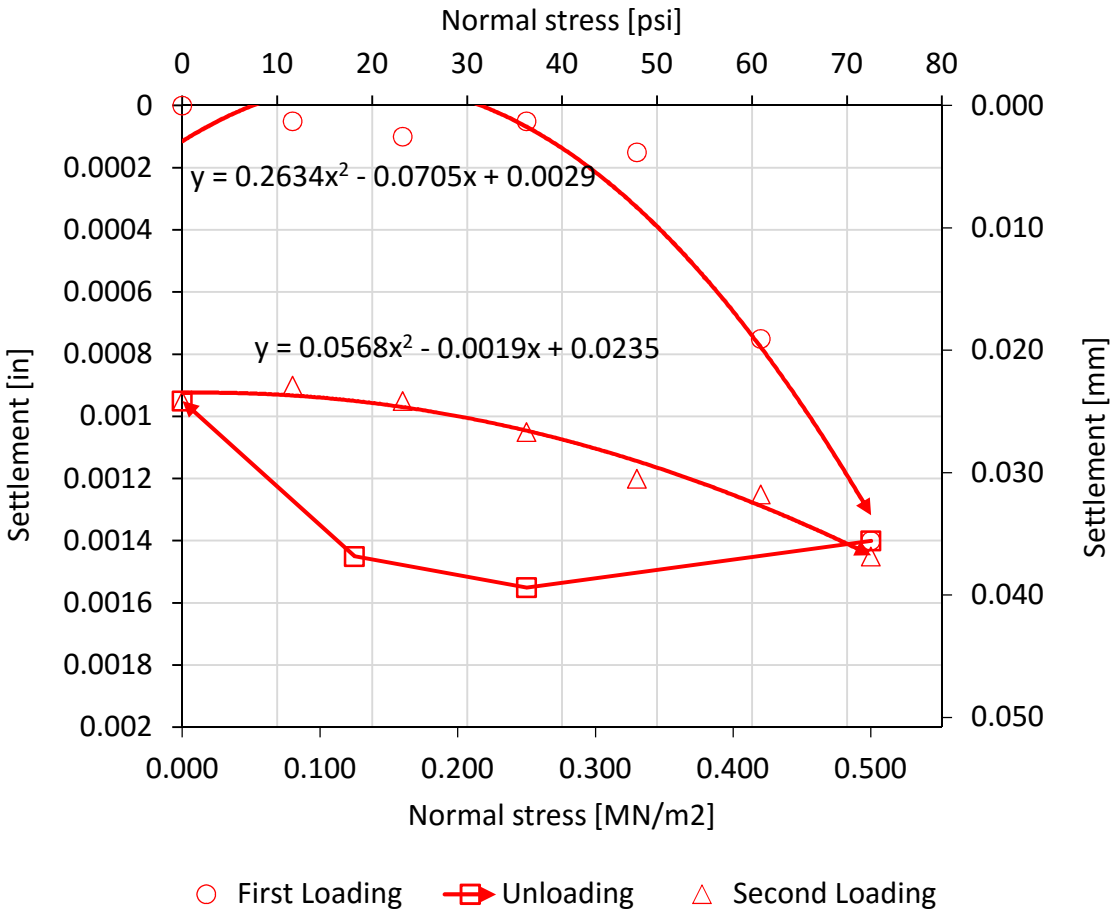

Figure 3-4. Plate deflection versus normal stress.

3.1.5 CTA Cylinders Unconfined Compressive Strength

CTA test cylinders were compacted into Proctor test molds during installation of the backfill for the 0˚, 30˚, and the 45˚skew test configurations for a total of 15 CTA cylinders. CTA was sampled from the chute of the mix truck in accordance with accepted sampling standards. Sampling was performed throughout the placement process to provide samples as representative as possible of the entire CTA zone.

Cylinders were compacted to 95% relative compaction in general accordance with the modified Proctor standard (ASTM 1557) on the rigid surface of the pile cap. Between lifts, a Casagrande grooving tool was used to striate the surface to facilitate bonding between the CTA layers. The cylinders were extruded using a hydraulic extruder immediately after casting. The samples were then sealed in pre-labeled zipper storage bags and placed in a shaded box for initial curing. After 48 hours, the cylinders were moved to the fog room where they finished curing, still in their sealed bags.

Seven days after casting, the cylinders were soaked in a water bath at room-temperature for a minimum of four hours, then capped with gypsum. The cylinders were then loaded into the compression machine and two linear variable differential transformers (LVDTs) were placed on opposite sides of the cylinder to monitor compressive displacement. The cylinders were then loaded at a strain rate of 0.02 inch per second until a significant reduction of load occurred.

Using the 0.2% offset method, the average UCS for the 15 cylinders was 1030 psi (7110 kPa) with a standard deviation of 500 psi (3470 kPa). Significant variation in UCS is to be expected in the field, due to factors such as differences in cement application rates, moisture content, and time between mixing and compaction. Even in the best field conditions, experienced

contractors have approximately a 40% standard deviation in cement application rates (Guthrie and Rogers 2010).

3.2 Installation and Quality Control of Backfill

Before the installation of the embankment backfill, work was necessary to prepare the testing apparatus. During installation, quality control was carried out to ensure the specified degree of backfill compaction was met.

3.2.1 Installation

The embankment backfill was placed and compacted inside in a 6 ft. (1.8 m) deep box running around 32 ft. (9.8 m) northward from the north face of the pile cap. For the side walls of the box, 2 ft. by 2 ft. by 6 ft. (0.6 by 0.6 by 1.8 m) pre-cast concrete blocks were placed to a height of 6 ft. (1.8 m) with compacted sand as backfill outside the blocks. Plywood sheeting 0.5 in. thick (1.3 cm) was then attached to the block wall and a layer of plastic sheeting was stapled to the plywood, as shown in Figure 3-5. The plastic was lubricated with cooking spray and a second layer of plastic was placed on the first, but not attached in order to allow free movement of the second plastic layer and minimize interface side friction.

To keep the space between the east and west pile cap and skew wedges free from debris, boards were placed in the gap and sealed with expanding foam. After installation and curing, the boards were removed to allow free movement of the pile cap.

Figure 3-5. Box side wall covered with plywood and first layer of plastic.

For the 30˚ skew test, a 15˚ reinforced concrete wedge was placed against the pile cap by crane and held in place by six 1 in. diameter and 1 ft. long (2.5 cm diameter and 0.3 m long) steel rods embedded in holes in the adjoining pile cap and concrete wedge faces. A second 15˚ concrete wedge was again joined to the first by steel rods for a total skew angle of 30˚. To further minimize vertical or transverse movement of the wedges, steel plates were attached to the top and sides of the blocks. The 45˚ skew test required removal of one of the 15˚ concrete wedges and the placement of a 30˚ concrete wedge attached by the same methods to the 15˚ skew wedge face.

To minimize base friction, the concrete wedges were placed on platforms consisting of 8 in. by 8 in. railroad ties with a 0.5 in-thick plywood sheets on top. The railroad ties and plywood were constructed to match the footprint of the skew wedge blocks. Base fabrication is shown in Figure 3-6.

Figure 3-6. Skew wedge base fabrication.

Lengths of 1 in. (2.5 cm) diameter steel pipe were placed on top of the platform parallel to the north pile cap face, as shown in Figure 3-7. The pipes were cut to appropriate lengths to act as rollers to reduce friction under the skew wedges during testing. To keep the space between the skew wedge and the wooden platform free from debris, plastic sheeting was taped to the base of the skew wedge to cover the gap between the bottom of the wedge face and the platform. In this way, the rollers were more able to roll freely.

Figure 3-7. Galvanized steel pipe rollers being installed on completed skew wedge bases.

Granular materials were stockpiled onsite and the CTA was mixed using a continuous concrete mixing truck. Because the mix truck was limited to a minimum of 5% cement, the specified 3% cement mix required special attention. For the 0˚ skew test, extra aggregate was weighed and added to the mixer for each batch in order to reduce cement content to 3%. This process is shown in Figure 3-8.

Figure 3-8. For 0˚ test, extra aggregate was added to each batch in order to meet cement content requirement.

For the 30˚ and 45˚ tests, the mix truck's standard amount of aggregate was used for each batch, but the cement hopper was emptied and the 3% cement weight was added manually which reduced manual labor considerably. Mixed CTA was placed into the bucket of a backhoe which then dumped the CTA in the box, shown in Figure 3-9. The same process was used for the Type 3 (gravel). The CTA and gravel was afterward spread by shovel to 6 in. (15 cm) lifts. Because of limited space, large compaction equipment was not an option; therefore compaction was accomplished using a combination of jumping jack compactors (Figure 3-10) and a remote controlled trench roller (Figure 3-11).

Figure 3-9. Backfill was dumped by backhoe into box, then spread by shovel before compaction.

Figure 3-10. Compaction was largely accomplished with use of jumping jack compactors.

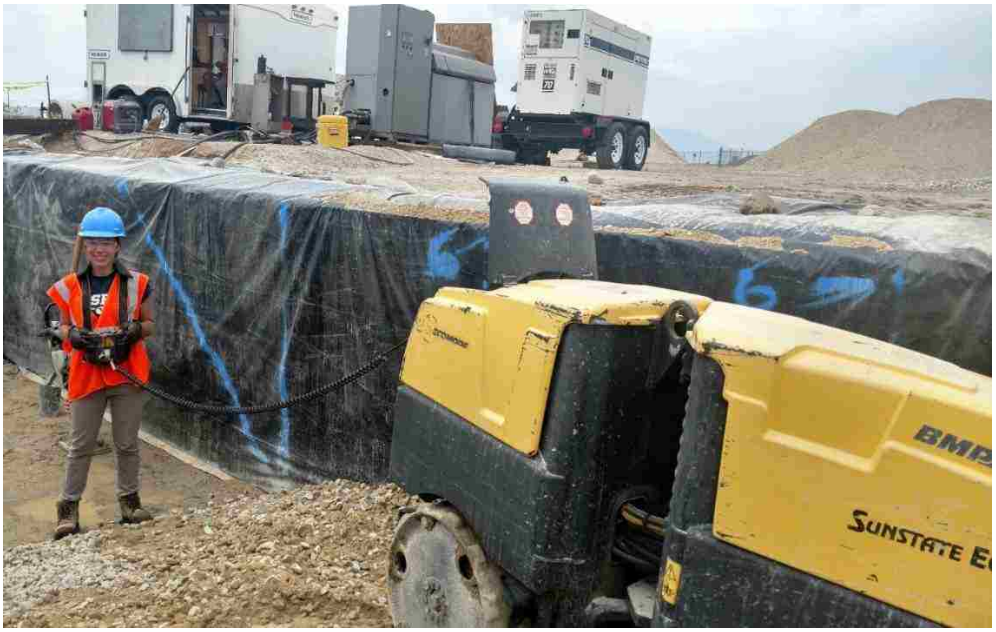

Figure 3-11. Rebecca Black operating a trench compactor.

3.2.2 Nuclear Density Tests

To assure compliance with California HSR specifications, density and water content in the compacted backfill was consistently monitored. Water content plays a crucial role in not only general compaction but also the eventual strength of CTA (Guthrie and Rogers 2010). Nuclear density gauges are less effective for materials containing cement because they work on the assumption that all hydrogen detected is in water molecules. As cement cures (or hydrates), hydrogen is taken from water molecules and integrated into cementitious molecules. Thus, as hydration progresses, a nuclear density gauge increasingly overestimates the moisture in the material. Dry density is then internally calculated by the gauge by subtracting the weight of water (calculated based on number of detected hydrogen atoms) from the measured wet density. Thus, because the gauge overestimates water content in cementitious material, the dry density is somewhat underestimated.

Despite the limitations of the nuclear density gauge, they are still used in standard industry practice; therefore, a nuclear density gauge was used for quality control testing during installation of the three testing configurations. Additionally, because of overwhelming industry precedent, although readings from a nuclear density gauge represent the wet and dry *unit weight* of the soil, the more conventional language of *density* is used.

Figure 3-12 shows a nuclear density test in process. As each lift of backfill was 6 in. after compaction, a 6 in. (15 cm) probe depth was used for density testing.

Figure 3-12. The author performing a nuclear density test.

Average results from the nuclear density testing are reported for the Type 2 (CTA) in Table 3-1, and for Type 3 (gravel) in Table 3-2 for each of the three testing configurations. As stated in section 3.1.2 Moisture-Density Relationship, the maximum dry density for the Type 2

(CTA) backfill was 138 lbs/ft^3 (21.7 kN/m^3) with an optimum moisture content of 6.5%, while the maximum dry density for the Type 3 (gravel) 135 lbs/ft^3 (21.2 kN/m^3) with an optimum moisture content of 6.5%. The relative compactions are percentages of the respective maximum dry densities.

Table 3-1. Type 2 (CTA) Average Values for 0º, 30º and 45º Testing Configurations

Test Configuration	Type 2 (CTA) Averages			
	Relative Compaction [%]	Moisture [%]	Moist Unit Weight pcf (kN/m^3)	Dry Unit Weight pcf (kN/m^3)
0˚	95.0	8.3	141.9 (22.3)	131.0 (20.6)
30˚	94.7	7.2	139.9 (22.0)	130.7 (20.5)
45˚	95.4	7.6	141.7 (22.3)	131.7 (20.7)

Table 3-2. Type 3 (Gravel) Average Values for 0º, 30º and 45º Testing Configurations

Test Configuration	Type 3 (Gravel) Averages			
	Relative Compaction [%]	Moisture [%]	Moist Unit Weight pcf (kN/m^3)	Dry Unit Weight pcf (kN/m^3)
0˚	97.4	6.6	140.2 (22.0)	131.6 (20.7)
30˚	97.4	6.6	140.2 (22.0)	131.5 (20.7)
45˚	96.8	7.5	139.6 (21.9)	130.7 (20.5)

For the 0˚ skew configuration, relative compaction, moisture content, moist unit weight and dry unit weight are plotted versus depth in Figure 3-13, Figure 3-14, Figure 3-15, Figure 3-16, respectively for Type 2 (CTA) and Type 3 (gravel) backfill zones. In each plot, blue points and lines represent results for the CTA and red represents gravel. the individual nuclear density gauge values are represented by points. The averages of the results for both the CTA and gravel

are plotted as dotted lines in each figure. These average values are the same as those found above in the tables.

In general, the following graphs show a trend that passing relative compaction values (relative compactions exceeding 95% of maximum dry density) are more common in the granular Type 3 (gravel) material. This may be a result of the issue, already discussed, with using a nuclear density gauge on cementitious materials. Because the nuclear density gauge's moisture measurement is based on hydrogen in the soil, the presence of hydrated cementitious molecules in the CTA gives an inaccurately high moisture reading, which is then subtracted from the wet density reading to calculate a dry density. Because of the exaggerated moisture measurement, the dry density reading is therefore inaccurately lower than the true dry density. On the other hand, because the granular material has no cement, it gives a more accurate reading of moisture, and therefore a more accurate calculated dry density.

Regarding Figure 3-13, the initial lift for the 0˚ test configuration embankment, located at elevation 0 ft. (0 m), had a series of non-passing tests (four points below 95% relative compaction). The relative compaction was poor because of the low density and high moisture content of the underlying native material. Increased compaction effort yielded no increase in density, so the decision was eventually made to accept the lower relative density and place the following lift. Despite the initial trouble, the average values, for relative compaction of the CTA meet the California HSR specification of 95%, even when conservatively including the extra two failing density tests from the first lift.

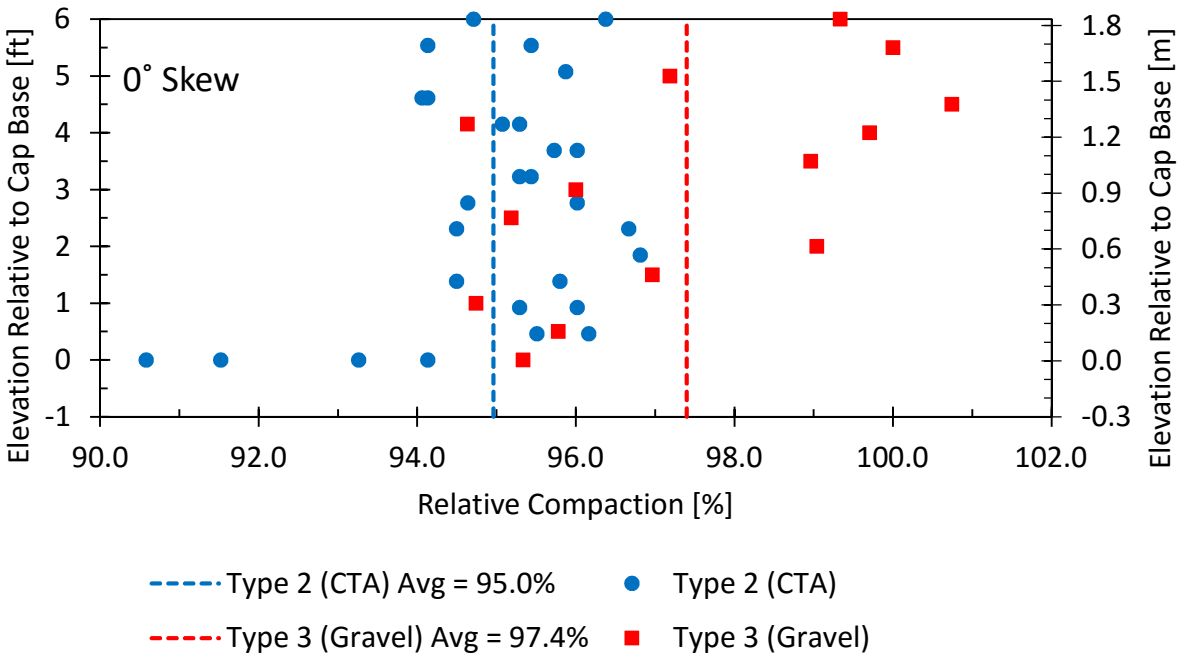

Figure 3-13. Depth versus relative compaction of backfill for 0˚ skew test.

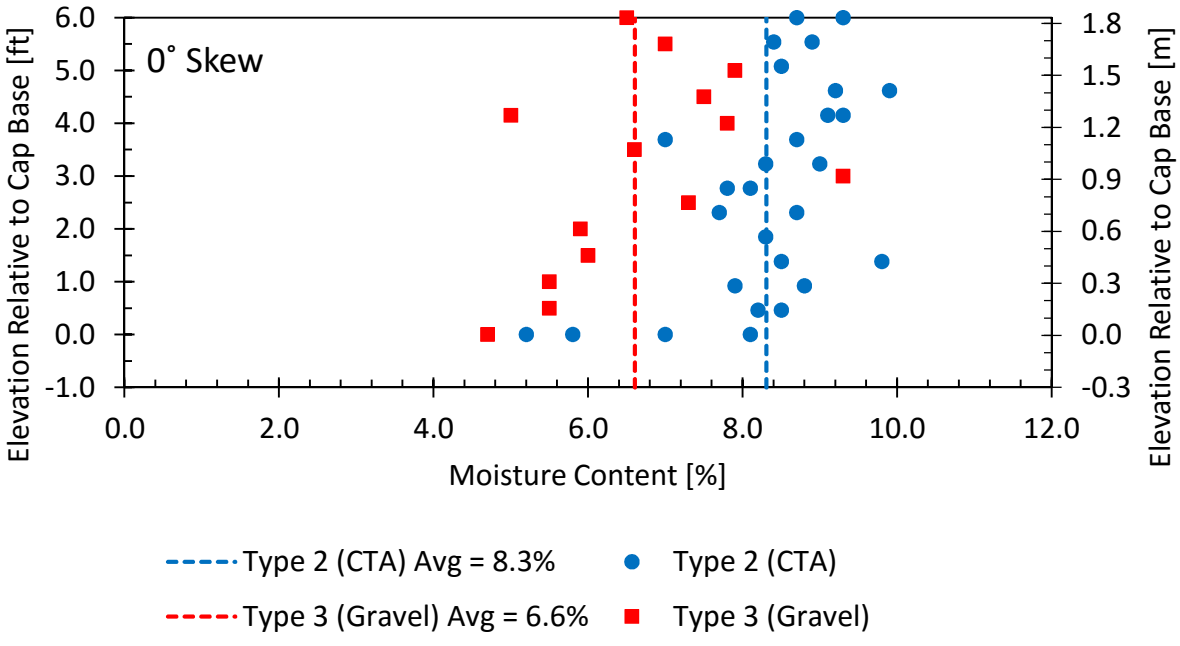

Figure 3-14. Depth versus moisture content of backfill for 0˚ skew test.

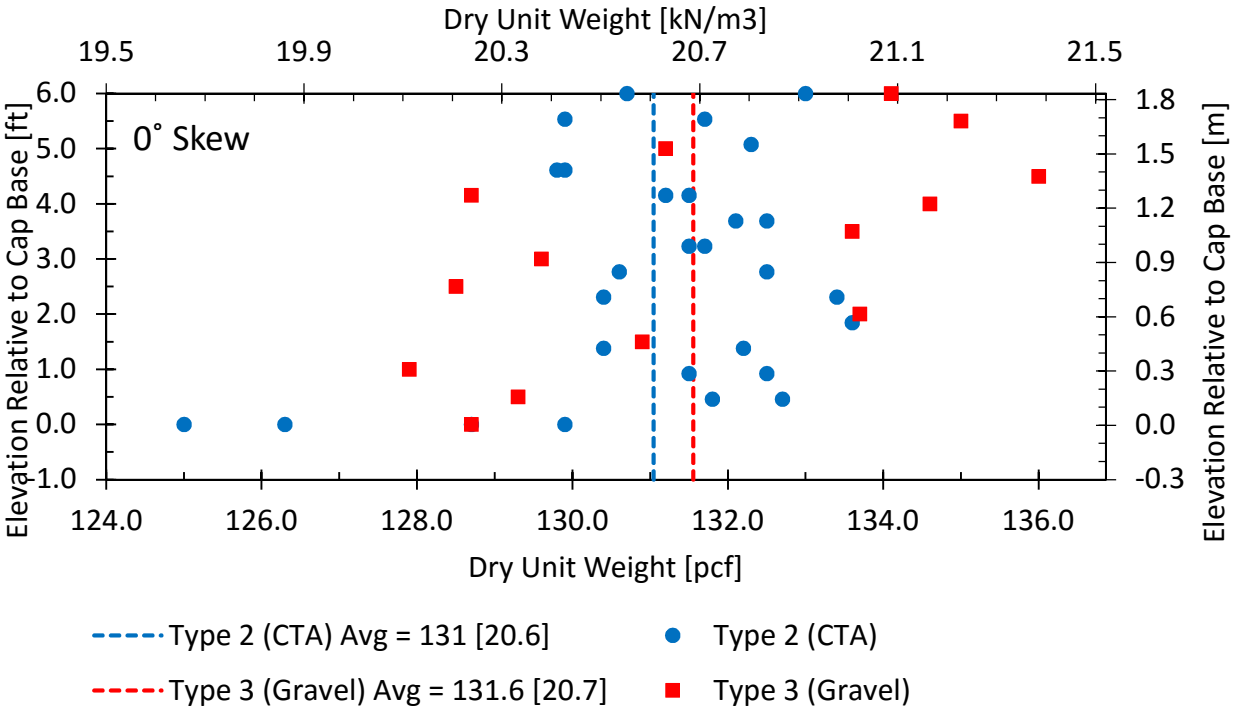

Figure 3-15. Depth versus moist unit weight of backfill for 0˚ skew test.

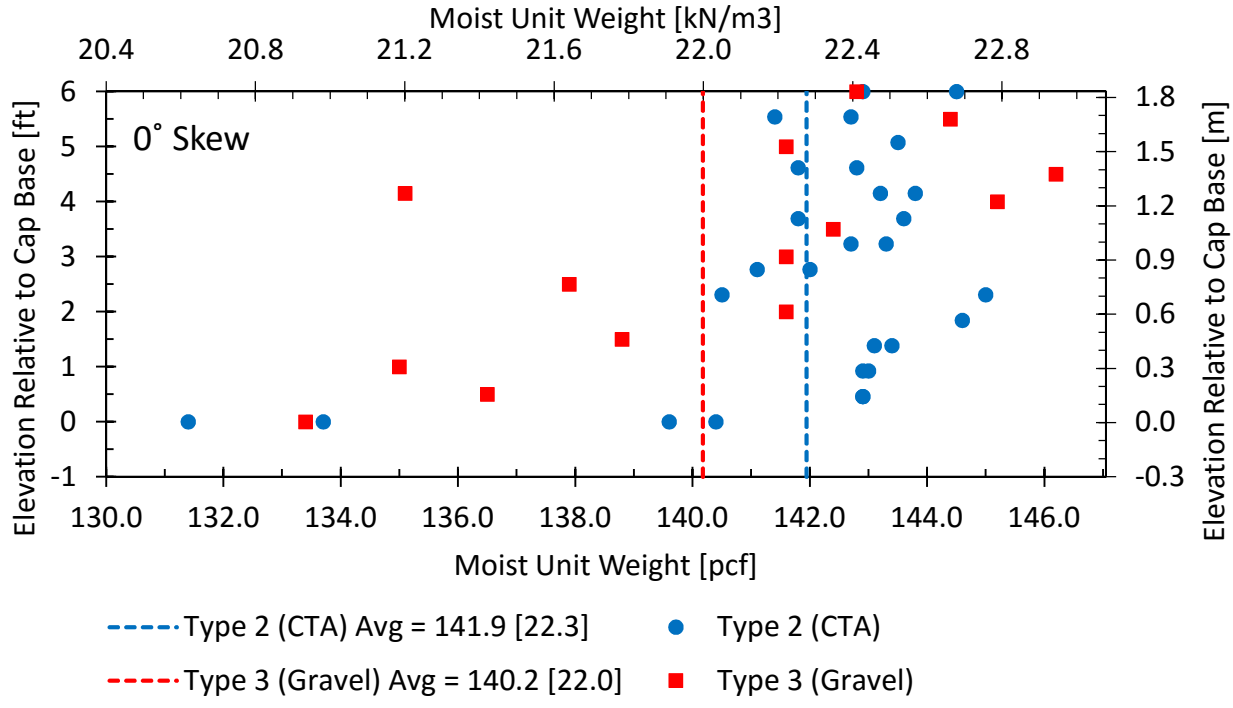

Figure 3-16. Depth versus dry unit weight of backfill for 0˚ skew test.

Similarly, for the 30˚ skew configuration, relative compaction, moisture content, moist unit weight and dry unit weight were plotted vs. depth for the CTA and gravel materials in Figure 3-17, Figure 3-18, Figure 3-19, and Figure 3-20, respectively.

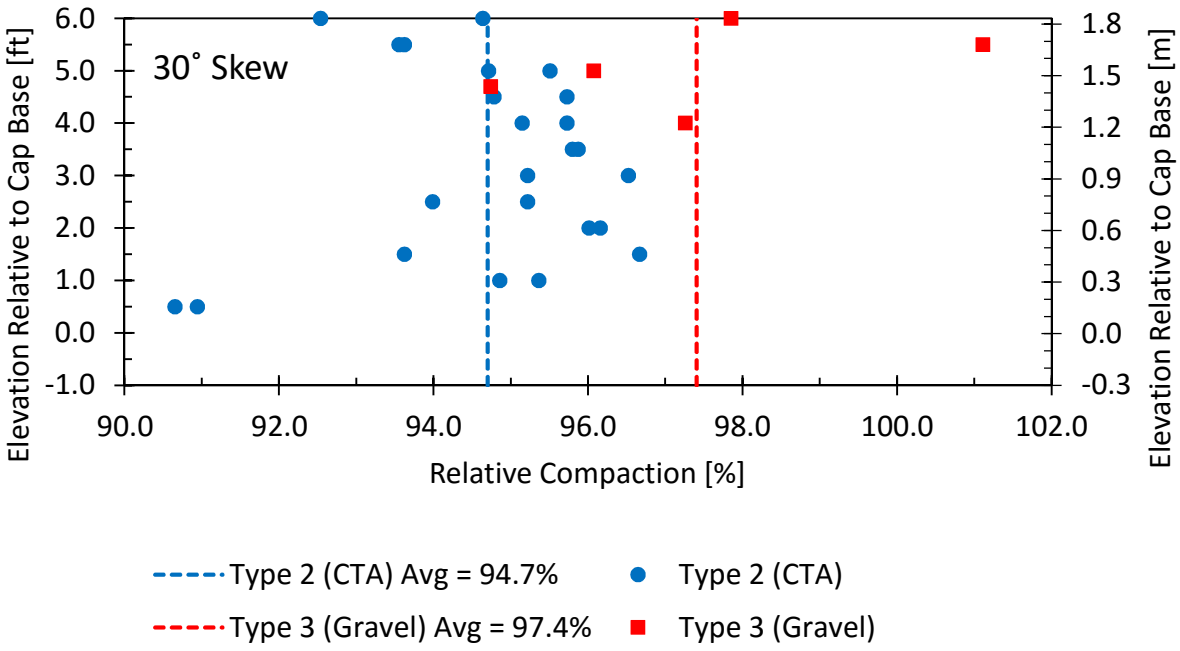

Figure 3-17. Depth versus relative compaction of backfill for 30˚ skew test.

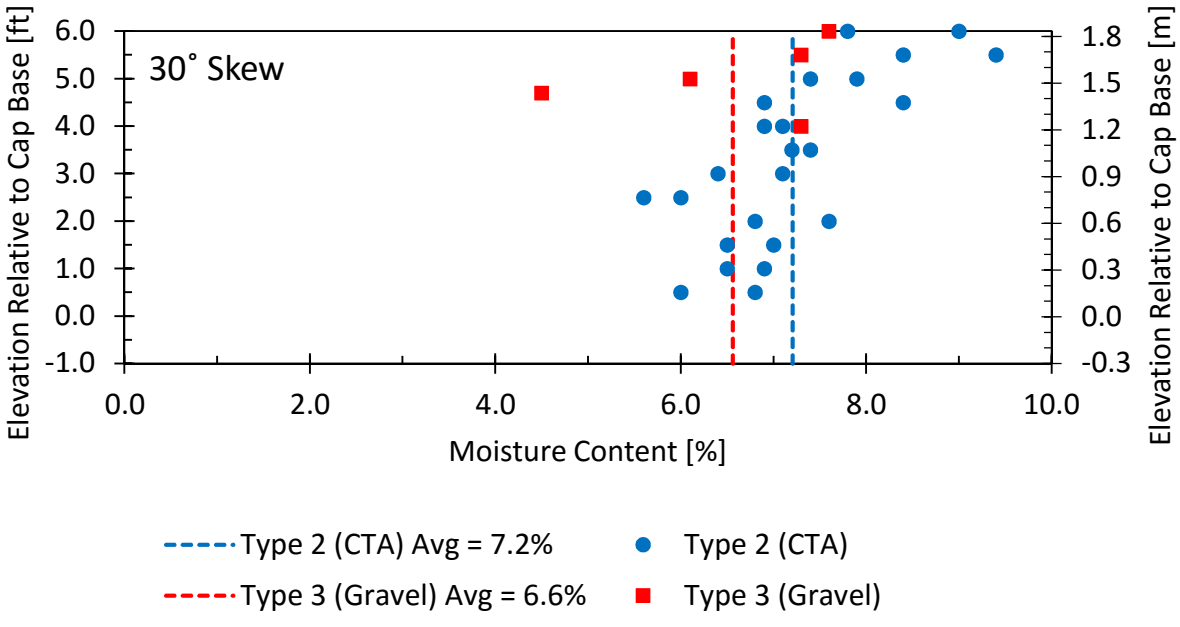

Figure 3-18. Depth versus moisture content of backfill for 30˚ skew test

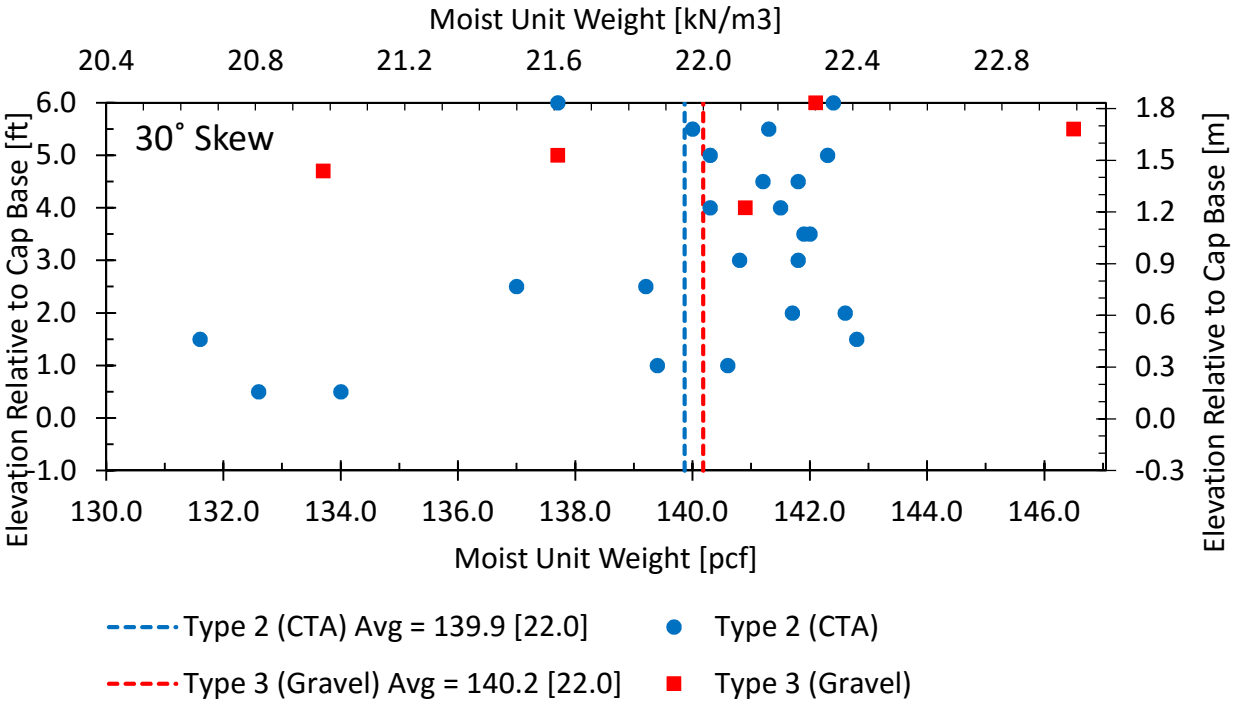

Figure 3-19. Depth versus moist unit weight of backfill for 30˚ skew test.

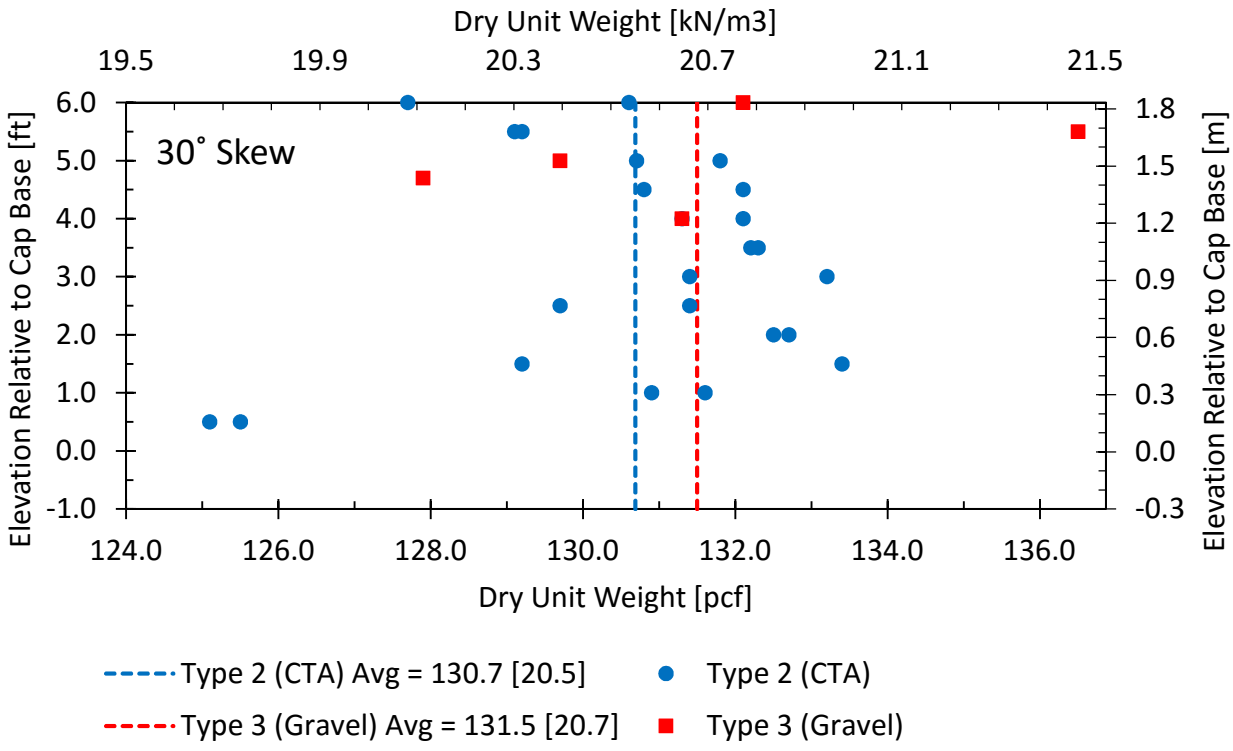

Figure 3-20. Depth versus dry unit weight of backfill for 30˚ skew test.

Finally, for the 45˚ skew configuration, the same plots were prepared for relative compaction, moisture content, moist unit weight, and dry unit weight in Figure 3-21, Figure 3-22, Figure 3-23, and Figure 3-24, respectively for the CTA and gravel backfills. Generally, the specified average minimum densities and moisture contents were within acceptable ranges.

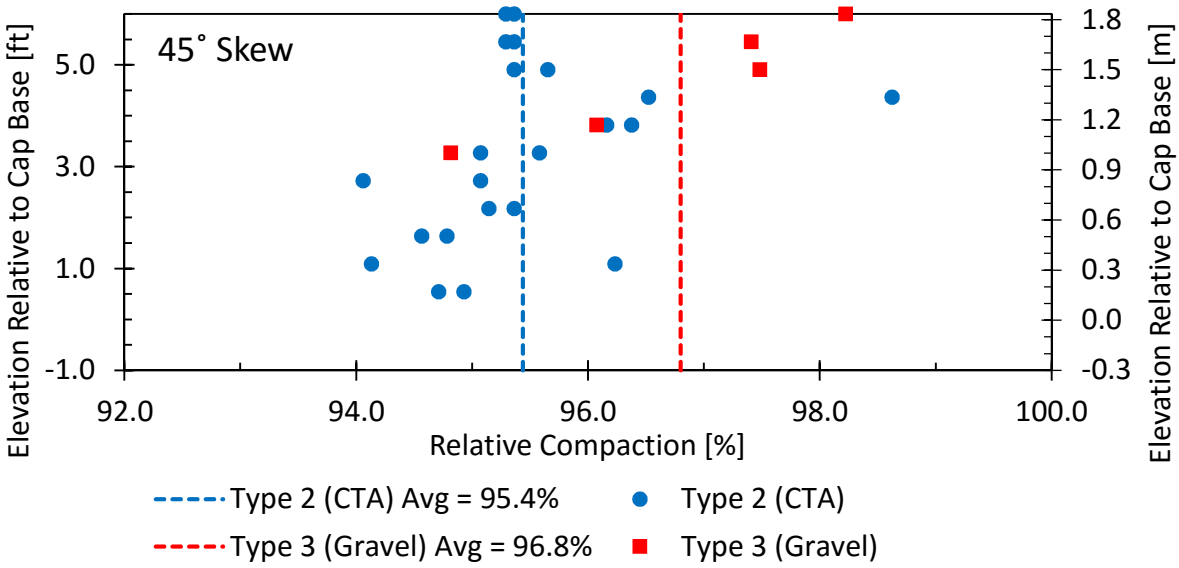

Figure 3-21. Depth versus relative compaction of backfill for 45˚ skew test.

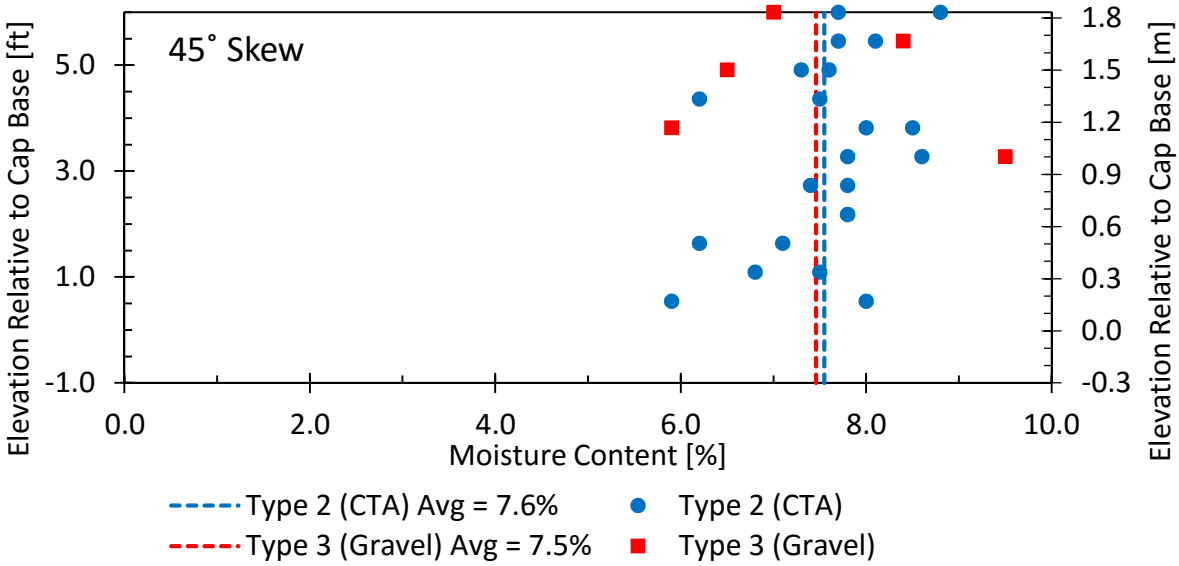

Figure 3-22. Depth versus moisture content of backfill for 45˚ skew test.

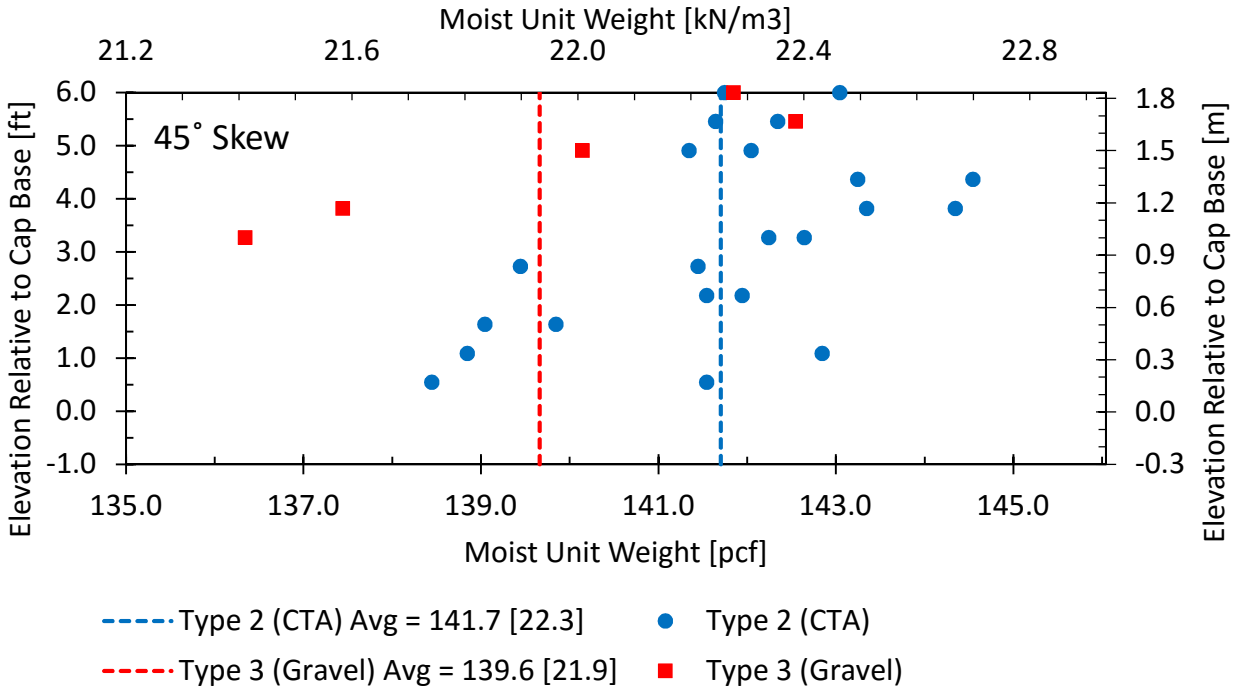

Figure 3-23. Depth versus moist unit weight of backfill for 45˚ skew test.

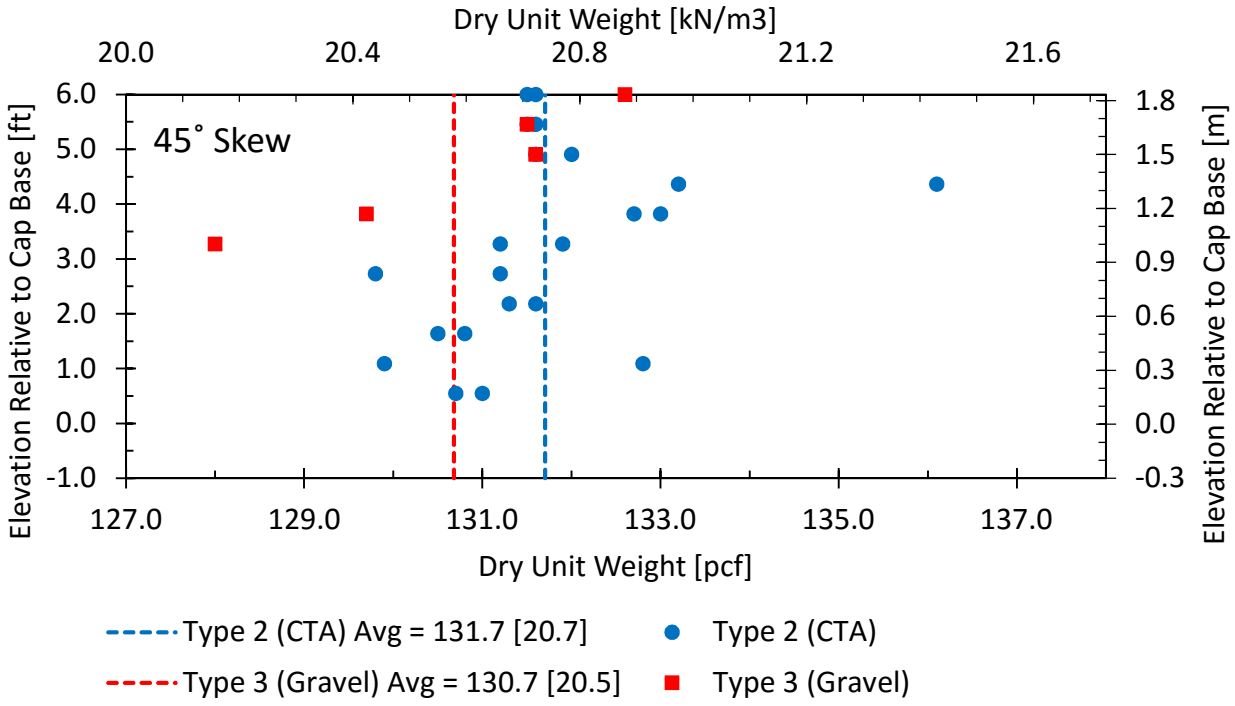

Figure 3-24. Depth versus dry unit weight of backfill for 45˚ skew test.

3.3 Passive Force Testing

The 0º, 30º and 45º test configurations were tested to failure under passive force. Passive force-deflection curves were created and plots of backfill heave and displacement were developed. Subsequently, back-analysis was carried out to determine if measured passive force could be adequately predicted using simple models which would facilitate future design.

3.3.1 Passive Force vs. Deflection Curves

The longitudinal force is the sum of the load applied by the two actuators. While the two actuators were equipped to collect displacement data as well, the displacement included movement at both the pile cap and the reaction frame against which the actuators pushed. For that reason, four string potentiometers (string pots) attached to an independent reference frame measured the pile cap displacement at the four corners of the pile cap face opposite the backfill. The pile cap displacement is the average of the four string pot measurements.

For each configuration, before construction of the CTA and gravel backfills, the actuators were used to push the pile cap about 4 in. (10 cm), a displacement greater than that necessary to cause the subsequent passive failure of the backfill. A force-deflection curve was created as a baseline of resistance exclusively from the piles and friction due to apparatus mass, including the skew wedges for the 30˚ and 45˚ configurations. Because the pile cap had been previously employed for a number of tests, the baseline resistance is relatively linear. This baseline resistance was then subtracted from the total load at the same displacement to obtain the net longitudinal force provided by the backfill alone. To determine the passive force, the longitudinal force is typically multiplied by the cosine of the skew angle, θ to resolve forces normal to the wall face (Burke, 1994).

The abutment load tests were conducted seven days after installation of the backfill to allow the CTA to cure prior to testing. The force-deflection plots for the 0˚ configuration in Figure 3-25 shows the baseline (no backfill) force-deflection curve, the total force-deflection curve, and the net longitudinal force (the total load minus the baseline). The baseline curve has been truncated to show only the force-deflection relationship in the deflection range of interest—from initial loading to failure.

As shown in Figure 3-25, the passive force developed for the transitional zoned backfill reaches nearly 800 kips (3.6 MN). This is significantly higher than the 300 kips (1.3 MN) that would be predicted for granular material using the Caltrans design procedure of 5 kips/ft^2 (0.24 MN/m^2) multiplied by the area of the backwall.

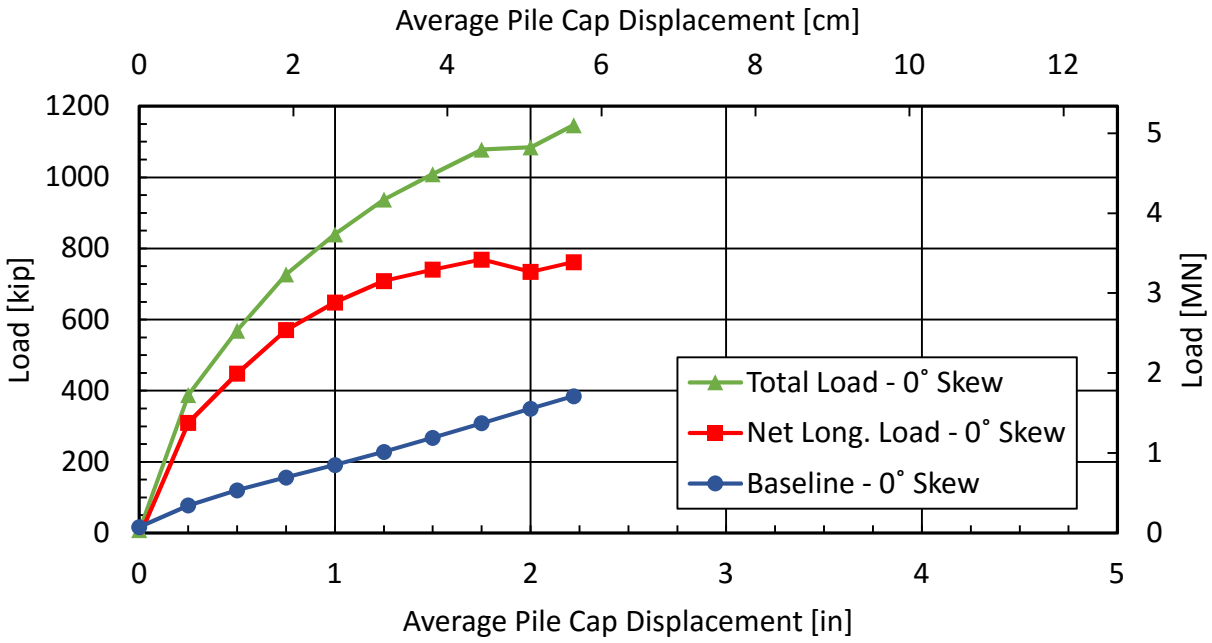

Figure 3-25. Total load, net longitudinal force and baseline load versus average pile cap displacement for 0˚ skew test.

Similarly, in Figure 3-26, the 30˚ test results are plotted, including the baseline, total load, and the net longitudinal load. The baseline curves in each skew test were relatively linear,

but the stiffness of the 30º and 45º curves was slightly higher than the 0º skew test, presumably owing to increased friction on the base of the concrete skew wedges.

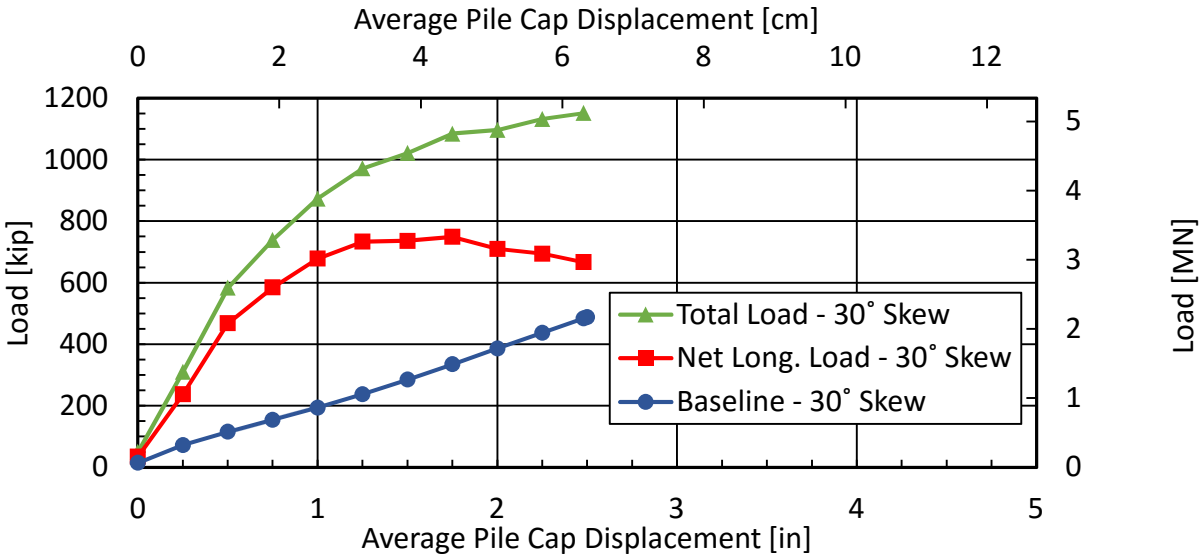

Figure 3-26. Total load, net longitudinal load and baseline load versus average pile cap displacement for the 30˚ skew test.

Finally, the 45˚ test configuration results are provided in Figure 3-27, with baseline, total load, and net longitudinal force curves.

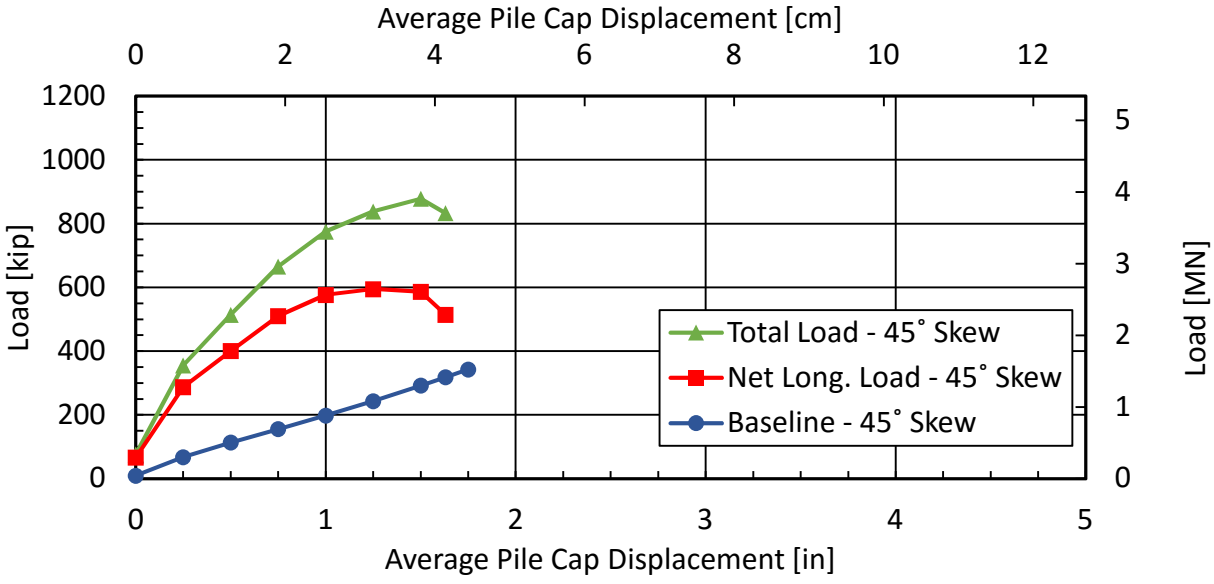

Figure 3-27. Load versus average pile cap displacement with total load, passive force, and baseline for 45˚ skew test.

Figure 3-28 provides a combined plot of the passive force (net longitudinal force multiplied by the cosine of the skew angle) versus displacement curves for the three skew angles for easy comparison. The plots in Figure 3-28 show that the three net longitudinal force-deflection curves have nearly identical initial force-deflection curves; however, when the curves begin to diverge, the 30˚ skew configuration develops slightly less peak capacity than the 0˚ skew, and the 45˚ skew has the lowest capacity of the three. The displacement necessary to mobilize the peak resistance also decreases as the skew angle increases. For example, peak resistance is mobilized at a pile cap displacement equal to about 3% times H for the 0˚ skew test, 2.3% times H for the 30˚ skew test, and 1.8% times H for the 45˚ skew test where H is the pile cap height of 66 inches (1.7 m). In contrast, for conventional granular backfills, the passive force is typically developed at a displacement equal to about 3 to 5% times H, which is somewhat higher than observed for the tests with the transitional zoned backfill.

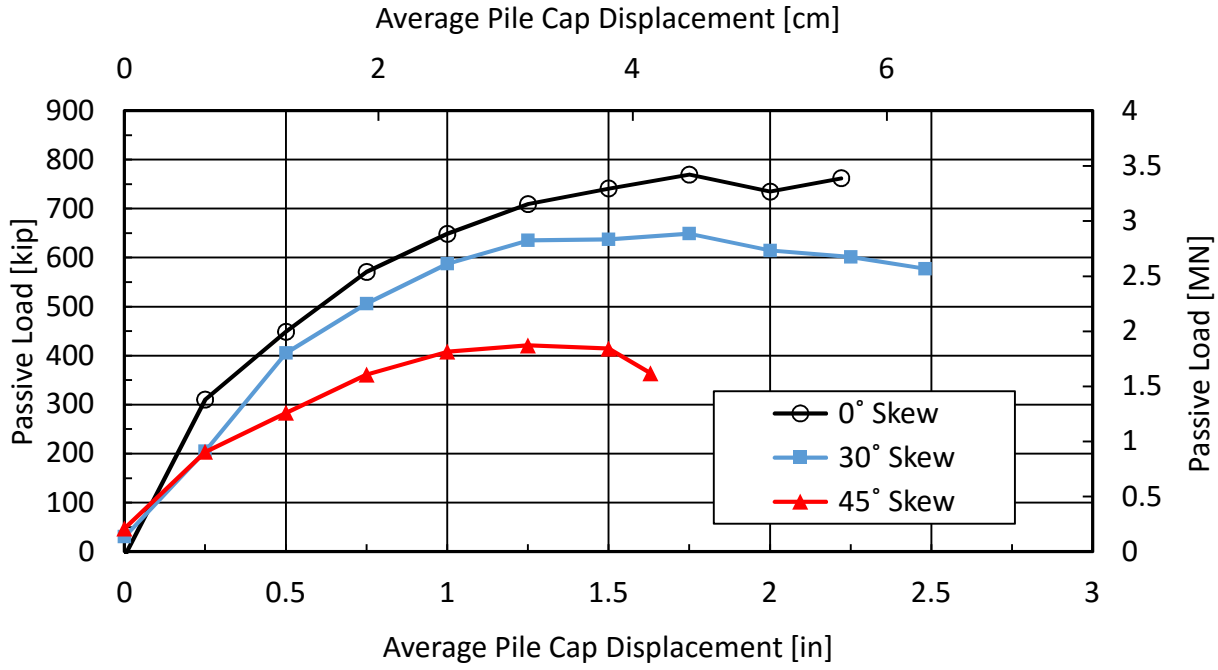

Figure 3-28. Combined plots for net longitudinal load curves for 0º, 30º and 45º tests.

Figure 3-29 provides a plot of the skew reduction factor (R_{skew}) as a function of skew angle based on the net longitudinal load and passive force obtained from the full-scale testing. At a skew angle of 30º, R_{skew} is about 0.83 for the transitional backfill whereas R_{skew} is predicted to be 0.51 for conventional sand and gravel backfills based on previous full-scale testing. Likewise, for a skew angle of 45º, R_{skew} is about 0.51 for the transitional backfill whereas R_{skew} is predicted to be about 0.37 for conventional sand and gravel backfills. These test results clearly show that there is less effect of skew angle on the passive resistance for the transitional zone backfill geometry investigated in this test series.

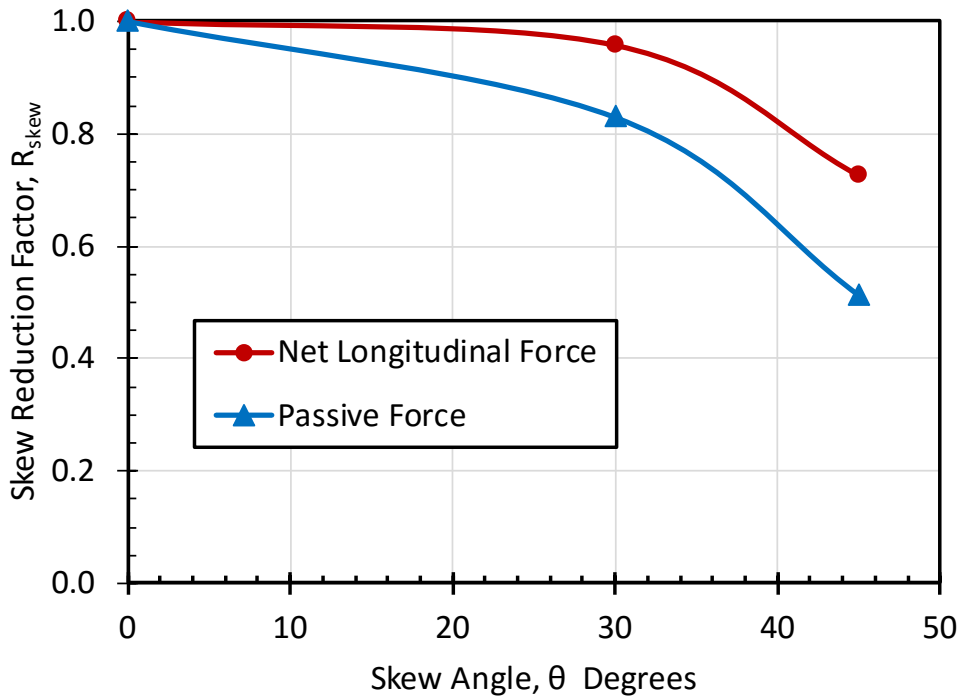

Figure 3-29. Skew reduction factor as a function of skew angle based on net longitudinal load and passive force.

3.4 Surface Displacement

Before and after passive force testing, elevation and horizontal location data over the embankment surface were gathered by digital level and total station. String potentiometers were installed on the embankment surface to gather data during passive force testing. The data from these three sets of instrumentation were processed to show heave and horizontal displacement trends.

3.4.1 Ground Heave Measurements with Digital Level

A 2 ft. (0.6 m) grid was spray-painted onto the surface of the backfill after backfill placement for each skew test. A digital level was then used to measure the elevation of each grid intersection before and after each load test. The final elevation values were then subtracted from the initial elevation values in order to give a value for change in elevation, or heave, for each grid intersection point.

In Figure 3-21, the heave data from the 0˚ test is represented in a color contour plot with the smallest heave represented by a dark green and the largest heave represented by red. Note that the largest heave is found in the Type 3 (gravel) zone. In contrast to tests on conventional backfill where the greatest heave occurred near the face of the cap, the CTA zone closest to the pile cap experienced the least heave. In fact, heave increased with distance behind the pile cap. This result suggests that the relatively stiff CTA backfill was largely displacing with the pile cap while a heave and failure were occurring in the gravel zone behind the CTA. No cracks are represented on the figure because none were observed within the spray painted grid zone; however, hairline cracks were noted just beyond the gridlines. Note that the scale for this plot is different than for the 30˚ or 45˚ plots.

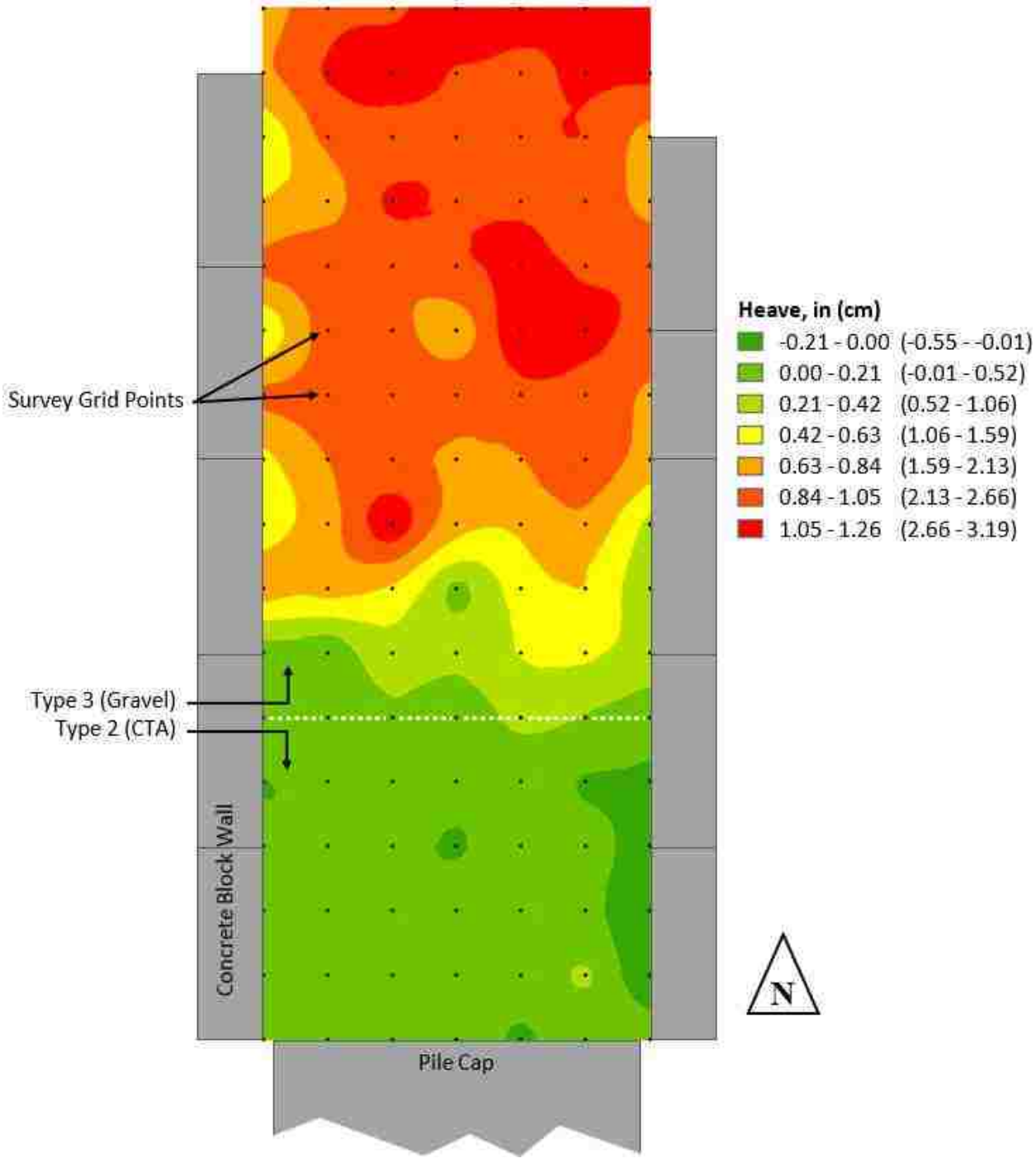

Figure 3-30. Heave from passive loading for 0° skew test.

The heave data for the 30˚ test is represented similarly in Figure 3-22, though the results are different from expected. Instead of the heave contours following the geometry of the backfill embankment, as seen above in the 0˚ skew and as seen later in the 45˚ skew, the heave for the 30˚ skew cuts across the CTA-gravel boundary. Nevertheless, the greatest heave occurred in the gravel backfill zone behind the CTA zone. Also, in contrast to other tests, visible shear cracks formed 3 to 4 ft. (0.9 to 1.2 m) behind the grid zone where the shear surface intersected the ground surface. Figure 3-31 is a photograph of the 30˚ skew embankment after passive failure, facing south. The green spray-painted line highlights the surface boundary between the Type 2 (CTA) and Type 3 (gravel) zones. The blue lines were spray-painted after the passive force testing along surface cracks where the passive failure surface was visible. This figure also shows the stakes placed at 2 ft. (0.6 m) increments to which string potentiometers were attached.

Figure 3-31. 30˚ skew after passive loading test, showing grid lines in orange and surface cracking highlighted in blue.

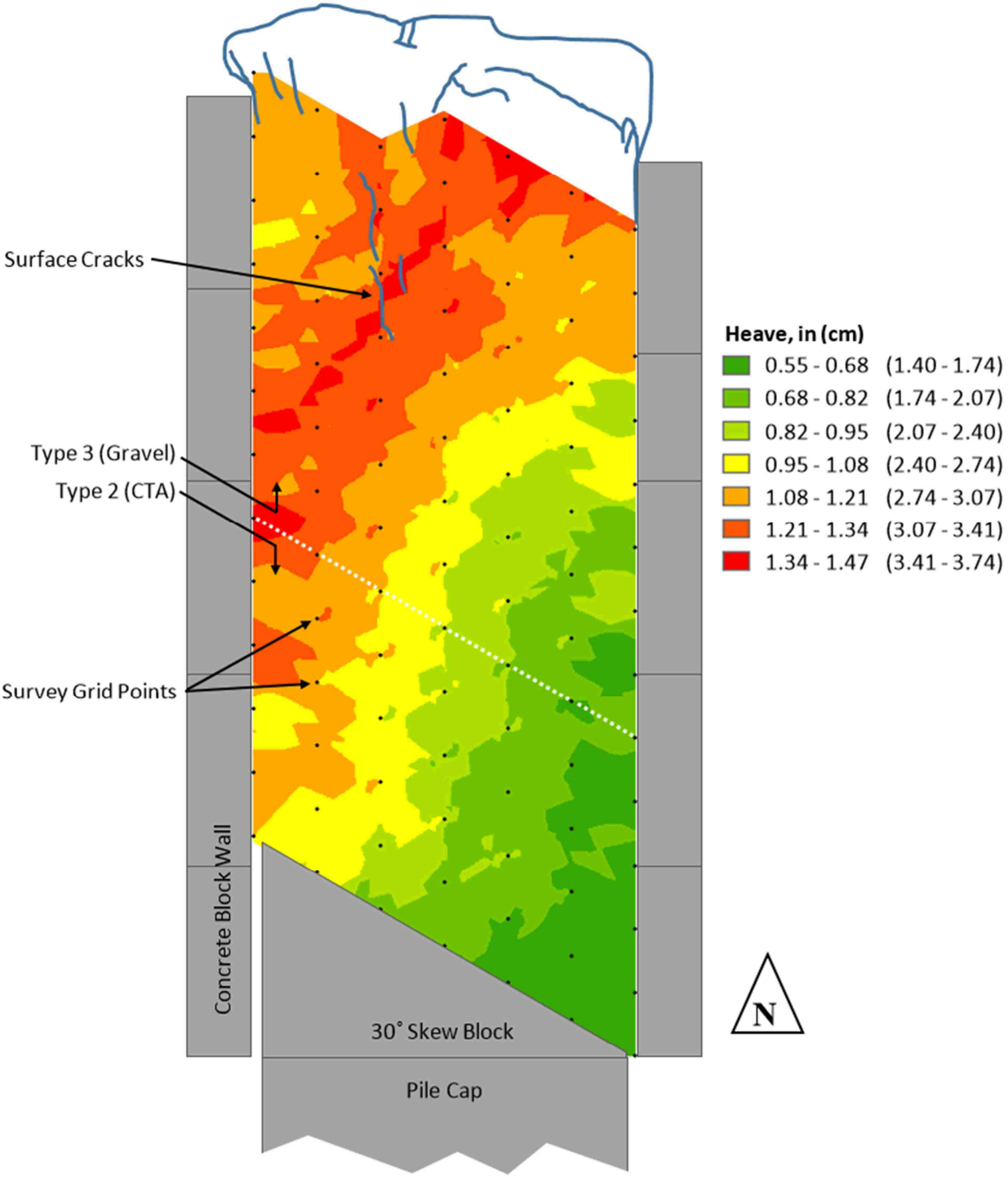

Figure 3-32. Heave from passive loading for 30˚ skew test.

Finally, the 45˚ skew heave data is presented in Figure 3-23. As mentioned previously, less heave was observed in the CTA zone and greater heave in the gravel zone behind the CTA. Note that the scale for this plot is different than for the 0˚ or 30˚ plots.

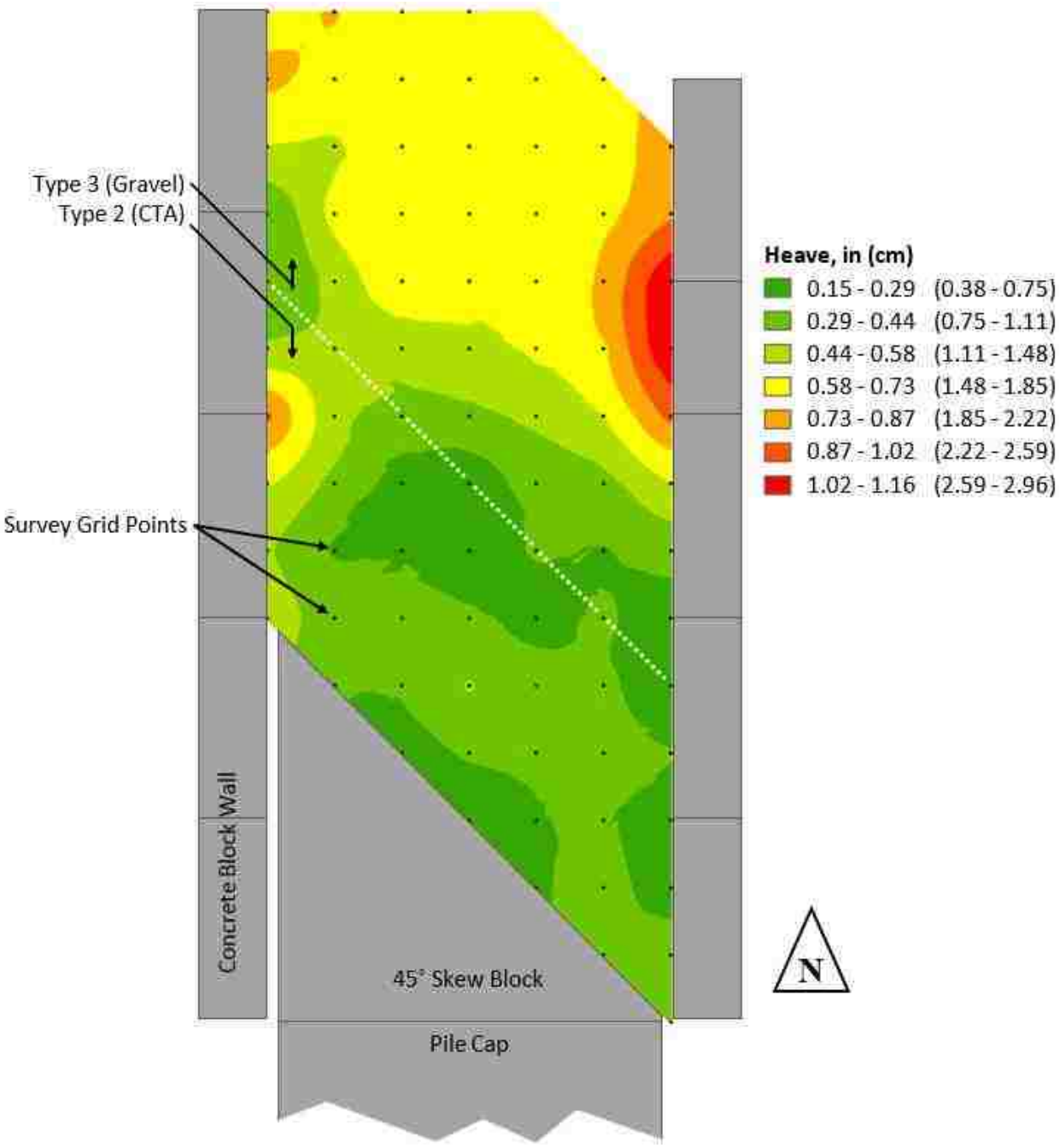

Figure 3-33. Heave from passive loading for 45˚ skew test.

3.4.2 Horizontal Ground Displacements from Total Station

Using the same grid intersection points as used for the digital level heave measurements, a total station was used before and after passive load testing to find the lateral displacement of the ground surface. Color contour plots were prepared to represent the magnitude of horizontal displacement. Figure 3-34, Figure 3-35, and Figure 3-36 show the color contours of measured displacement, with dark green representing smaller displacement and red representing larger displacement. Note that all three figures have differing color scales.

Because the color contours only communicate displacement magnitude, vector plots were also prepared using the same data. Figure 3-37, Figure 3-38, and Figure 3-39 are vector plots showing both the magnitude and direction of the horizontal displacement of the grid intersections for the 0˚, 30˚ and 45˚ tests, respectively. Vectors have been scaled up to improve readability, with arrows pointing in the direction of point displacement. Each vector line is color coded according to magnitude (green representing less displacement, red representing more displacement). Note that while the color scales differ from figure to figure, all three vector plot figures were subjected to the same scaling factor of 10, meaning the lines are ten times longer than the actual displacement recorded for each point.

Closely related to the trends shown in the heave plots (Figure 3-30, Figure 3-32, and Figure 3-33), the Type 2 (CTA) zone seems to have experienced the largest horizontal displacement, suggesting that the zone largely displaced as a block with the pile cap with little internal strain, as shown in the vector plots for the 0˚skew test in Figure 3-37, and color contour Figure 3-34. This can be seen by the fairly consistent displacement magnitudes in the Type 2 (CTA) zone, with decreasing magnitudes in the Type 3 (gravel) zone. In other words, it appears that the embankment failure occurred in the Type 3 (gravel) zone. Similar trends are less apparent but

still discernable with the 30˚ test (Figure 3-35 and Figure 3-38) and the 45˚ test (Figure 3-36 and Figure 3-39).

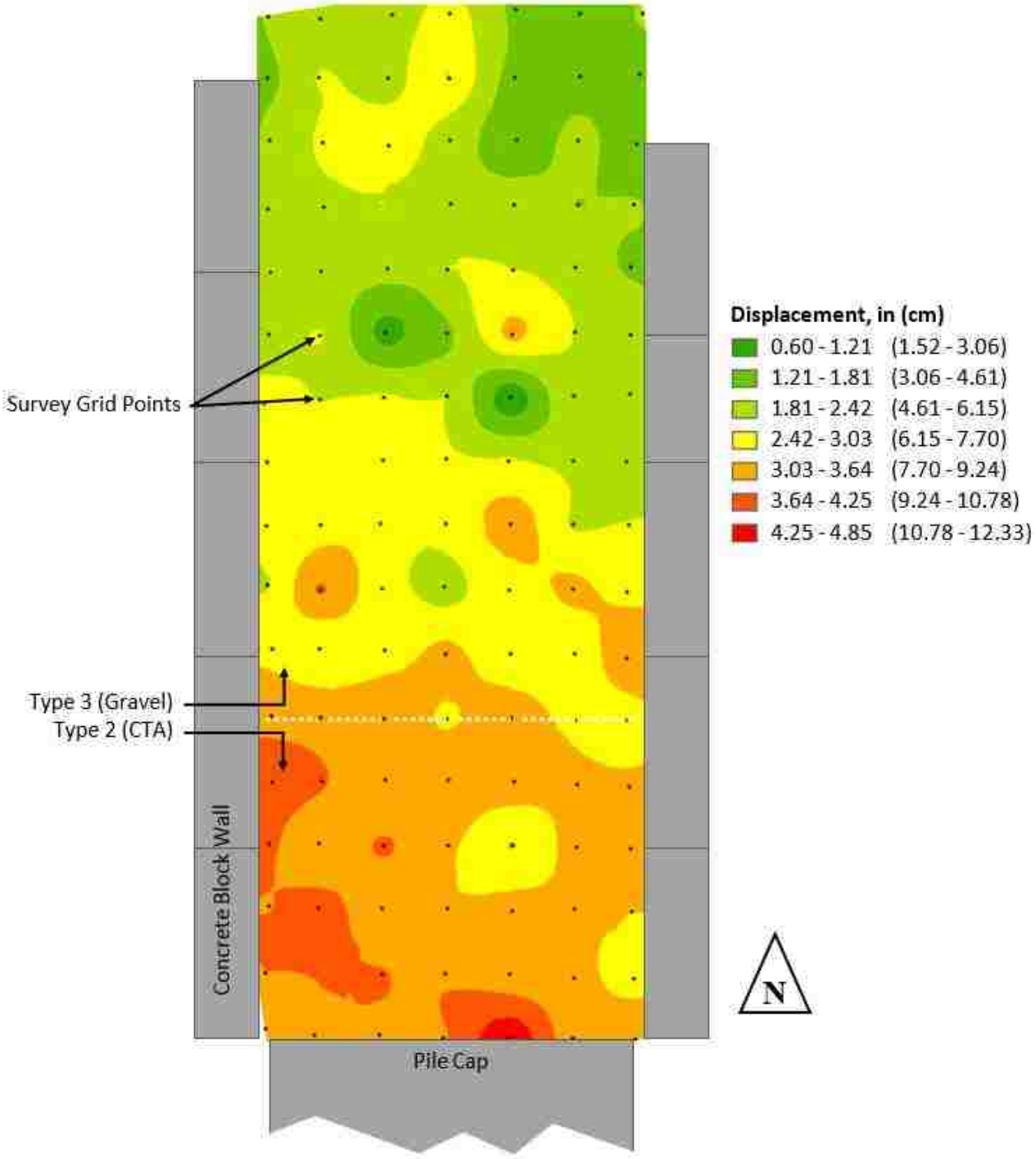

Figure 3-34. Horizontal displacement color contour for 0˚ test.

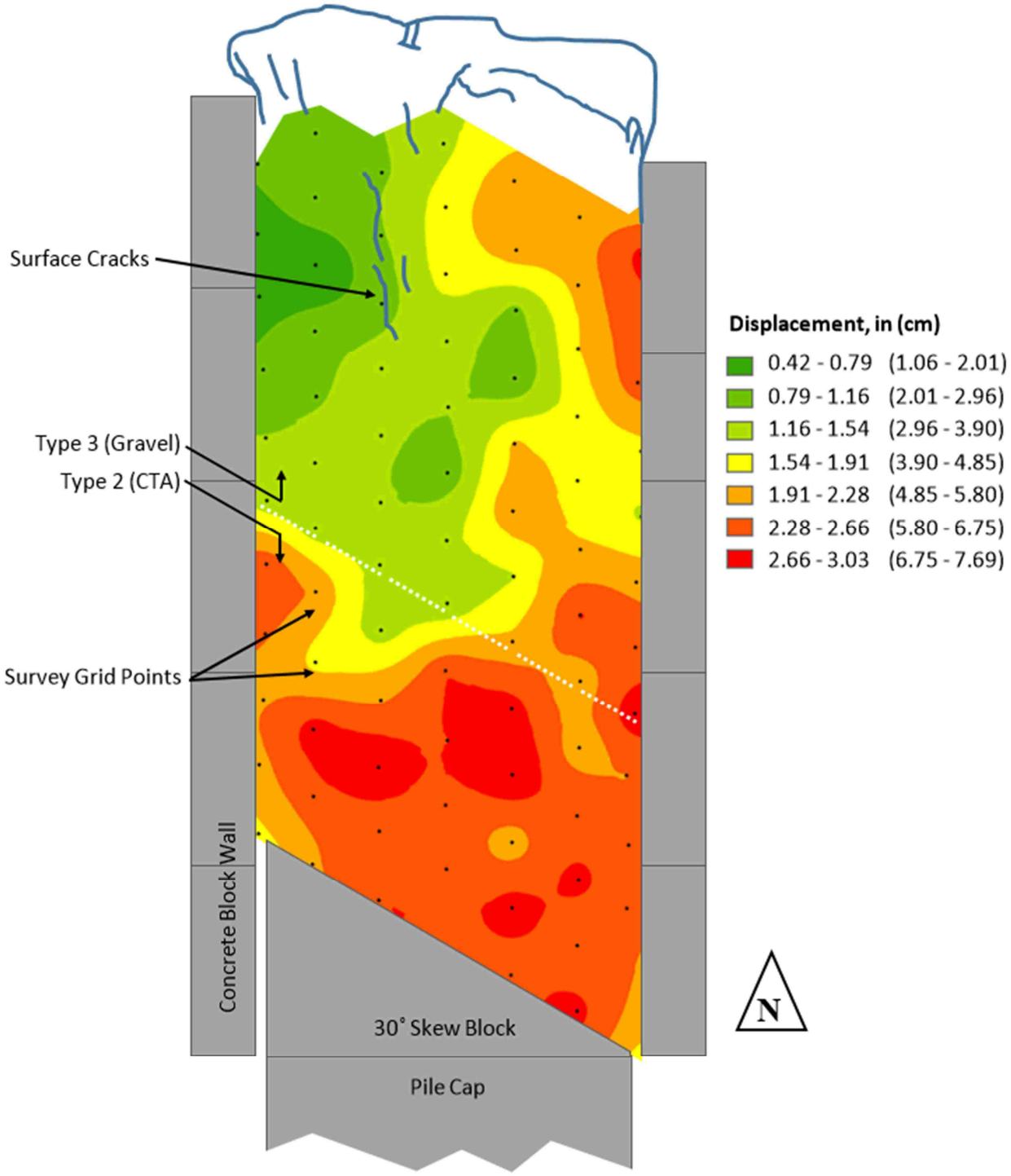

Figure 3-35. Horizontal displacement color contour for 30˚ test.

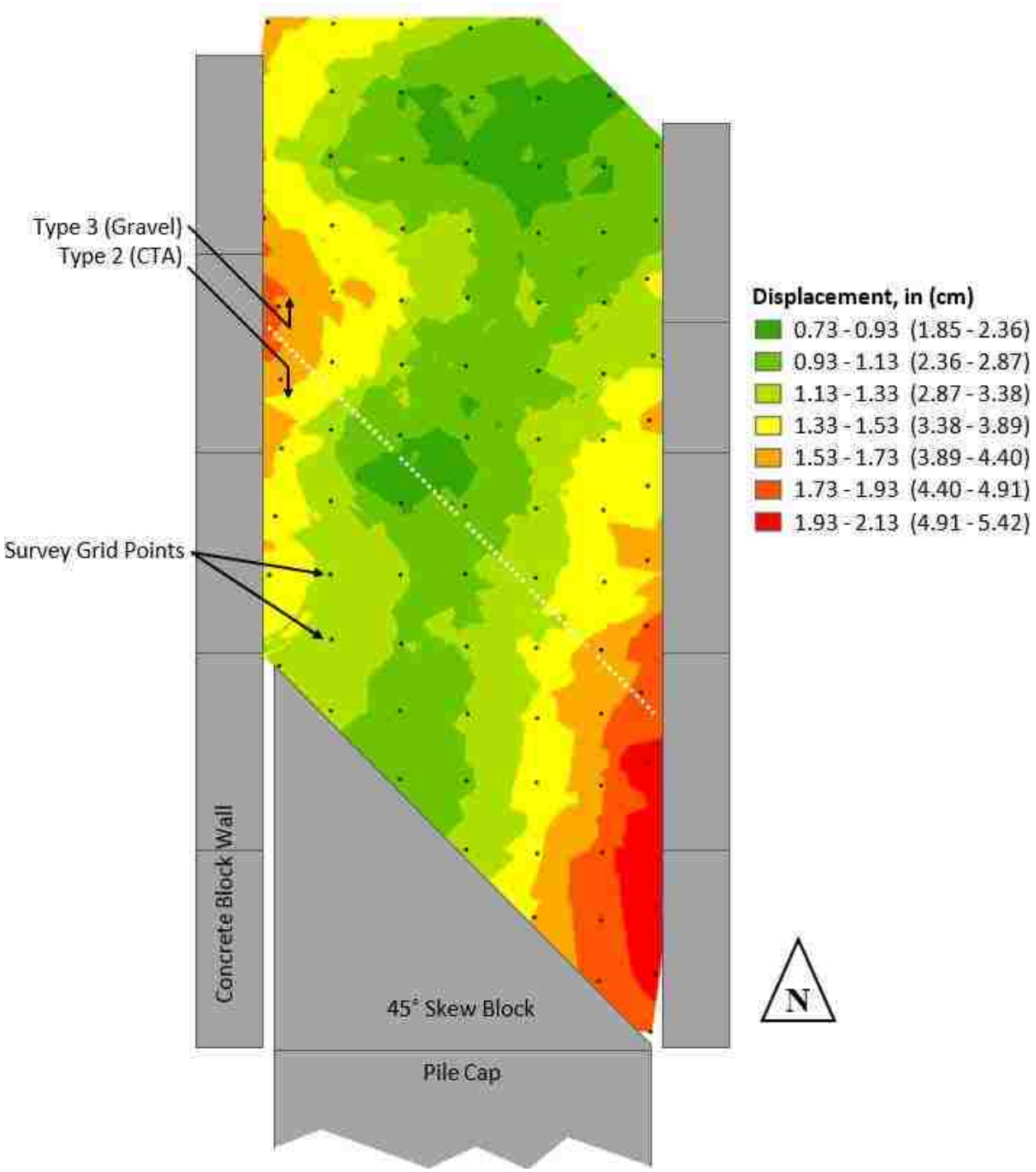

Figure 3-36. Horizontal displacement color contour for 45° test.

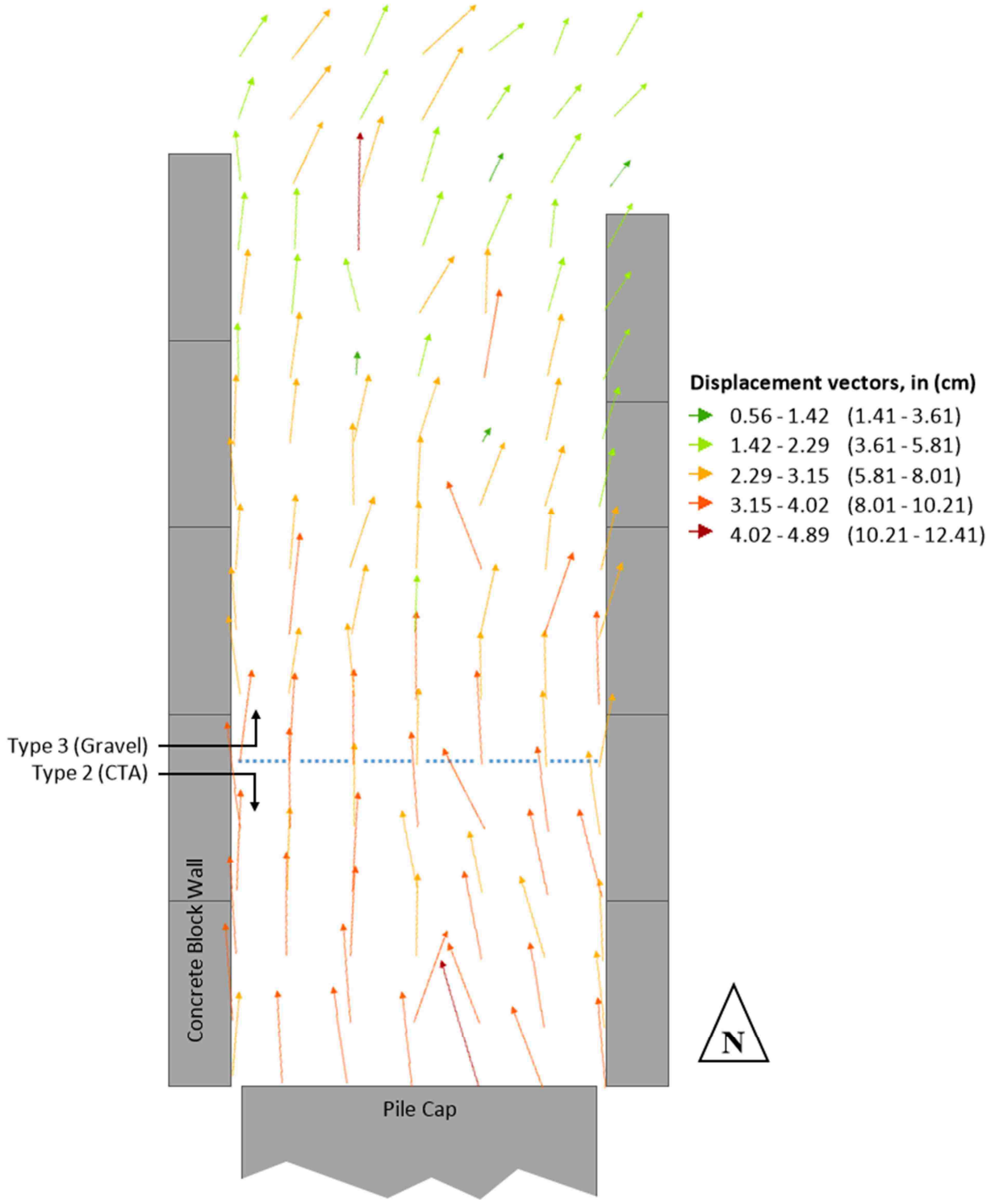

Figure 3-37. Scaled up horizontal displacement vectors for 0˚ test.

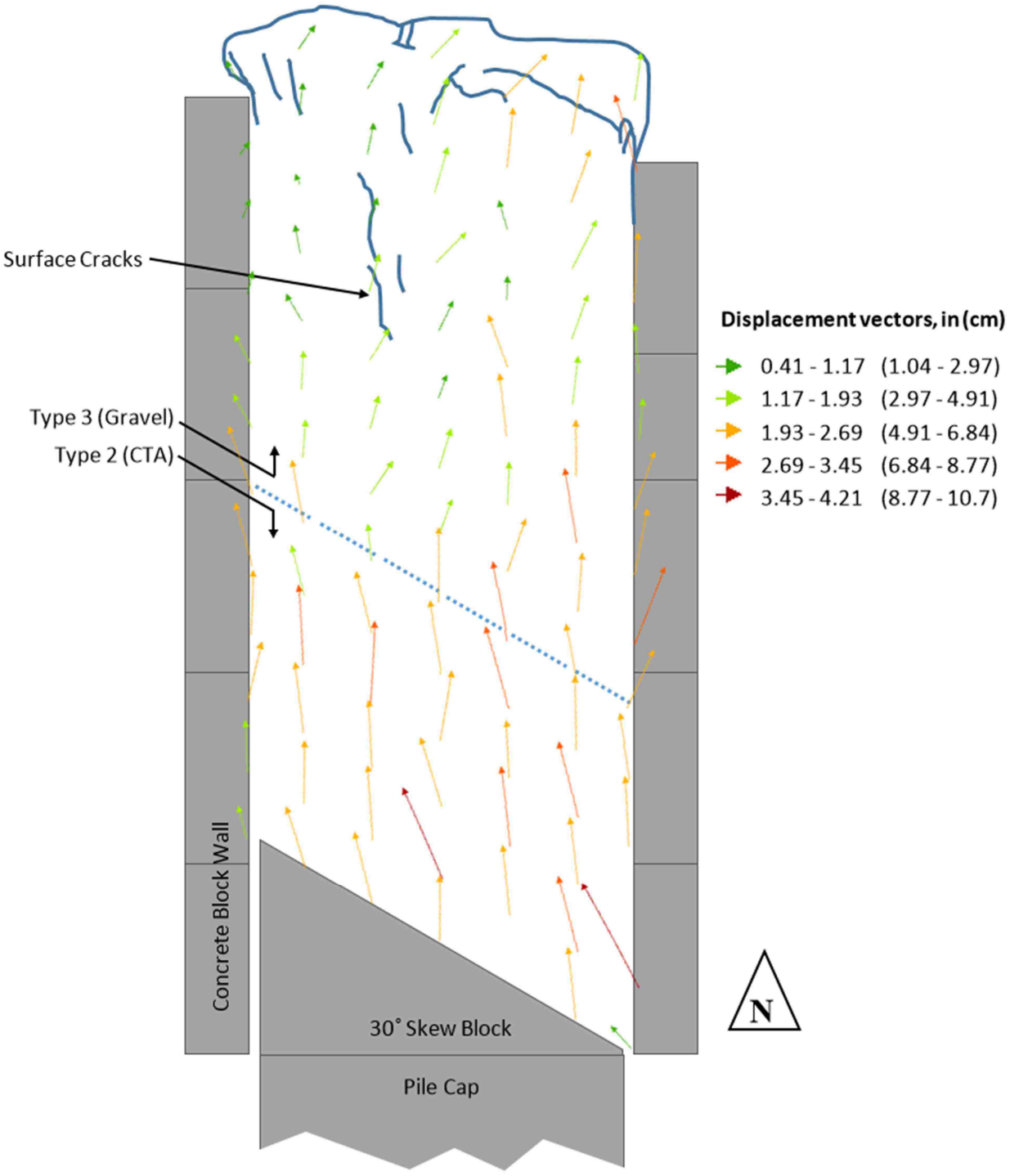

Figure 3-38. Scaled up horizontal displacement vectors for 30˚ test.

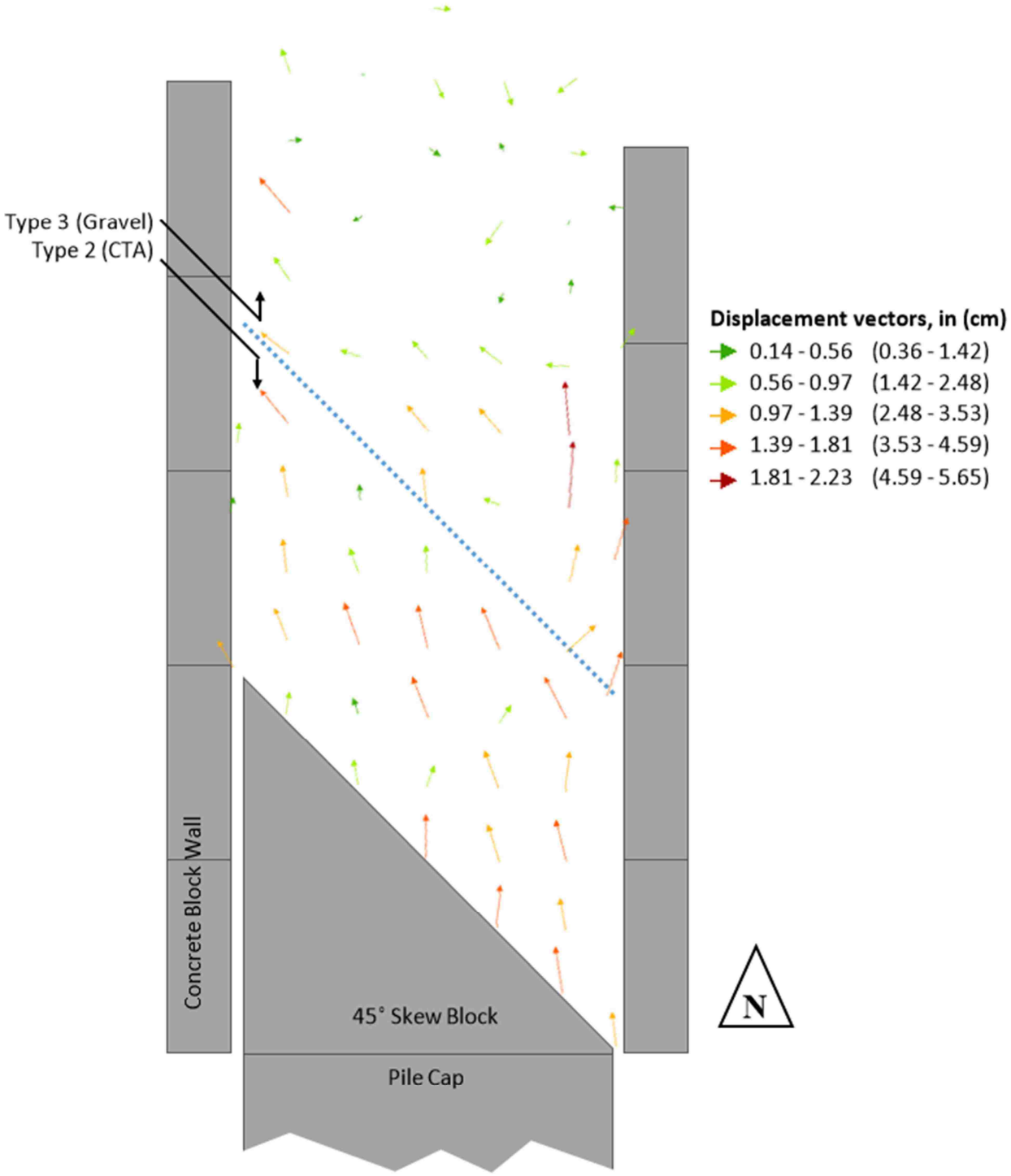

Figure 3-39. Scaled up horizontal displacement vectors for 45° test.

3.4.3 String Potentiometers

As an additional source of data regarding ground surface distortion, string potentiometers (string pots) were attached to stakes driven in the ground at regular intervals along the length of the backfill surface. These string pots were mounted to the top of the pile cap. The data was then used to calculate the average compressive strain in each interval. The strain data for the 0˚, 30˚, and 45˚ skew test configurations is represented in Figure 3-40. The average strain calculated for each 2 ft. (0.6 m) interval away from the pile cap face is plotted in different color and line type depending on the test configuration.

As shown in the figure, the strain is relatively small. Whereas similar testing with traditional gravel backfill has shown a maximum strain around 5% near the pile cap, the maximum strain for the transitional backfill geometry is only about 1.5%.

Higher strain in the 4 ft. (1.2 m) closest to the abutment is commonly observed and is most likely due to a combination of higher stress and inferior compaction in the zone immediately against the abutment back wall due to difficulty in maneuvering compaction equipment in close proximity to existing structures.

Negative strain is most likely error due to strain calculation for each interval being dependent on the displacement for that interval and on the preceding interval's displacement. Thus peaks are sometimes located adjacent to neighboring troughs, as shown in the final intervals for the 0˚ and 45˚ strain plots.

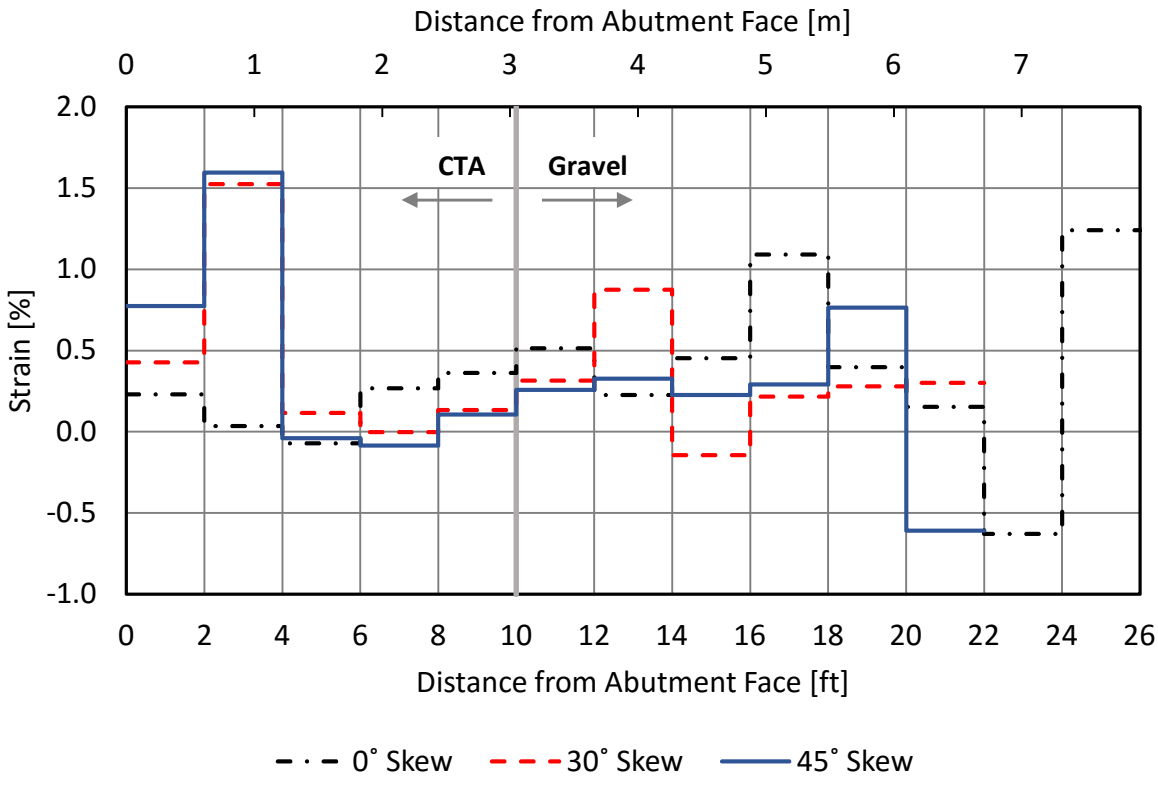

Figure 3-40. Average strain in each 2 ft. interval for 0º, 30º and 45º testing configurations.

3.5 PYCAP Analysis

After passive force testing was performed on the 0˚ skew backfill, the force-deflection curve was loaded into PYCAP, a spreadsheet program for computing force-deflection curves for backfills (Mokwa and Duncan, 2001). Assuming that failure occurred in the granular backfill zone (Type 2) and not the CTA zone, known values were input and assumed values adjusted until good agreement was found between the computed and measured force-deflection curves. A comparison between the measured and computed curves is provided in Figure 3-41 and the agreement is very good.

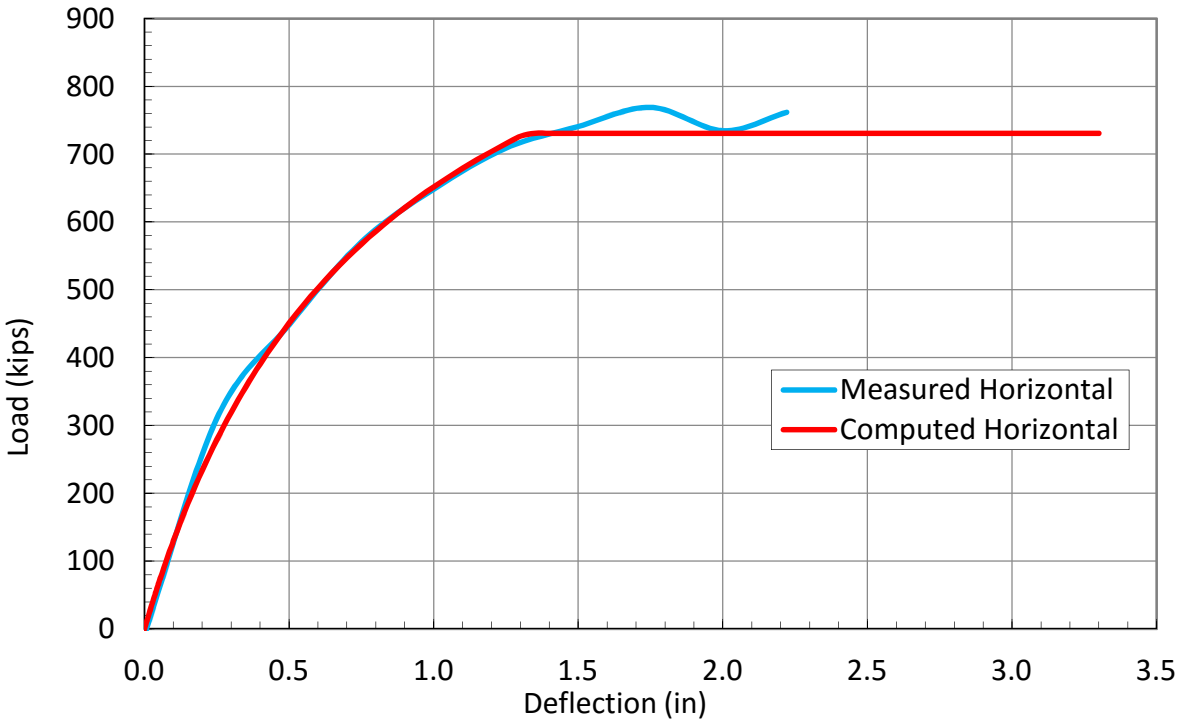

Figure 3-41. Measured and computed force-deflection curves for 0˚ skew assuming failure in granular Type 3 (gravel) zone.

The known and assumed values input into PYCAP are shown in Table 3-3. Most values are intuitive; however, a few parameters require additional explanation. The cap width is increased from the actual width to 11.5 ft. (3.5 m) to account for additional space between the pile cap and the sidewalls. The wall friction angle is often assumed to be 70% of the soil friction angle for gravel against concrete; however, because the wall in this case is the interface between the CTA and gravel backfill zones, it is more reasonable to assume that the wall friction angle is equivalent to the soil friction angle. This is because the two materials were compacted together and a rough interface developed as the CTA cured against the gravel backfill ensuring that failure would occur within the gravel backfill. The friction angle of the compacted gravel backfill is almost the same as the friction angle (45.8º) obtained from in-situ direct shear tests on similar backfill conducted previously at the test site by Frederickson (2017).

Table 3-3. Input Values for PYCAP Resulting in Computed Load-Deflection Curve Assuming Failure in Granular Type 3 (Gravel) Zone (Known Values in Bold, Assumed Values in Italics)

Input Description		Input Value
Cap width,	b (ft) =	**11.50**
Cap height,	H (ft) =	**5.50**
Embedment depth,	z (ft) =	**0.00**
Surcharge,	q_s (psf) =	**0.0**
Cohesion,	c (psf) =	**0.0**
Soil friction angle,	ϕ (deg.) =	*46.0*
Wall friction,	δ (deg.) =	*46.0*
Initial soil modulus,	E_i (kip/ft^2) =	*2500*
Poisson's ratio,	ν =	*0.25*
Soil unit weight,	γ_m (pcf) =	**140.2**
Adhesion factor,	α =	*1.00*
	Δ_{max}/H =	*0.02*

As an alternative assumption to the failure plane residing entirely in the granular Type 3 (gravel) zone, the failure surface may instead be assumed to have been entirely in the Type 2 (CTA) zone. Figure 3-42 shows the measured and computed force-deflection curves from PYCAP using this alternative assumption. Note that the same data are used in plotting the measured force-deflection curves in the both Figure 3-41 and Figure 3-42. The visual difference between the measured force-deflection curves in the two figures is due to the difference in the scale of the vertical axis. The computed curve Figure 3-42 has a maximum value around 3.5 times the measured maximum of around 800 kips.. The poor agreement between the computed and measured curves in Figure 3-42 and the very good agreement in Figure 3-41 strongly implies that the passive failure surface developed in the gravel behind the CTA zone rather than within the CTA zone.

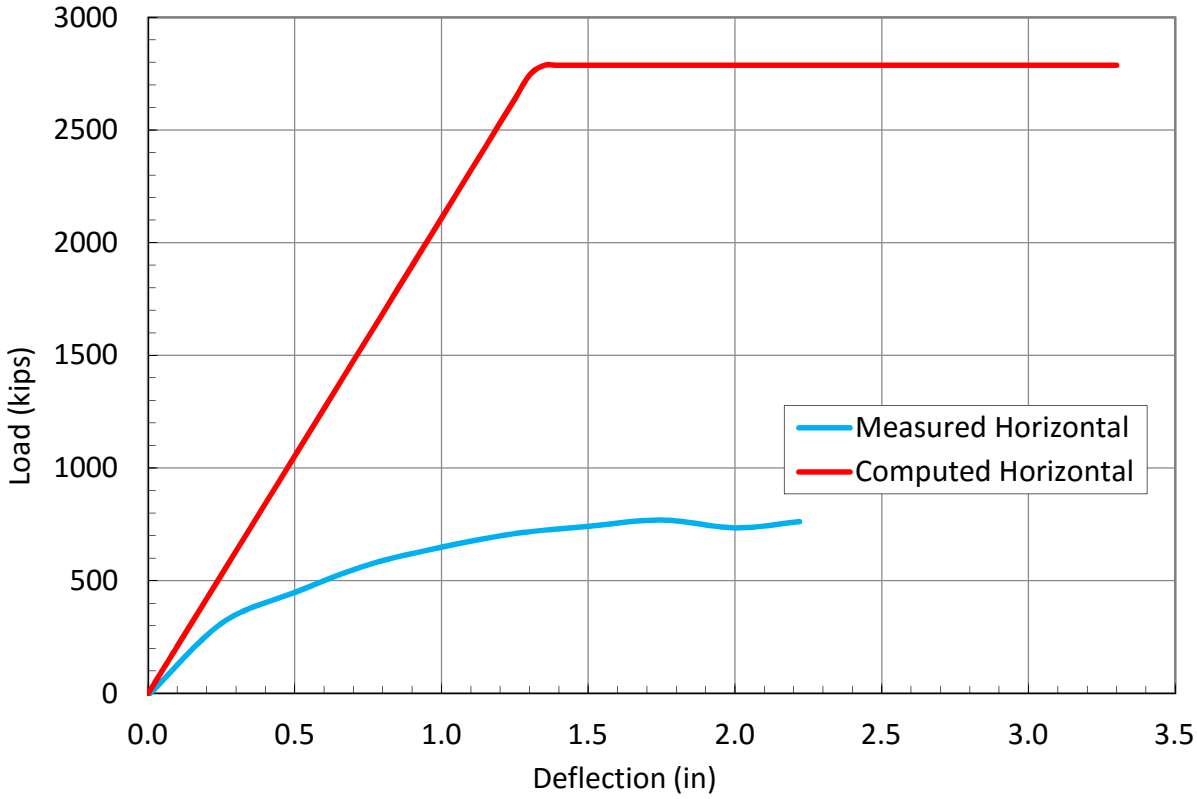

Figure 3-42. Measured and computed force-deflection curves for 0˚ skew assuming failure in the Type 2 (CTA) zone.

Table 3-4 shows the input values used to compute the force-deflection curve. Most are the same as shown in Table 3-3, but cohesion, soil friction angle, wall friction angle, and soil unit weight are different. The parameter for cohesion is often taken as half the material's unconfined compressive strength (UCS); however, as a more conservative assumption, tension strength (assumed to be 12% of the UCS) was used. The CTA, strongest in compression and weakest in tension, would not have realistically failed entirely in either tension or compression, so an all-tension failure offers a lower force-deflection curve than would be expected if the failure occurred in the Type 2 (CTA) zone. Soil and wall friction angles were assumed to be zero, and the average dry density of the CTA zone was used for the 0˚ skew test.

Table 3-4. Input values for PYCAP Resulting in Computed Load-Deflection Curve Assuming Failure in Type 2 (CTA) Zone (Known Values in Bold, Assumed Values in Italics)

Input Description		Input Value
Cap width,	b (ft) =	**11.50**
Cap height,	H (ft) =	**5.50**
Embedment depth,	z (ft) =	**0.00**
Surcharge,	q_s (psf) =	**0.0**
Cohesion,	c (psf) =	*28683.0*
Soil friction angle,	ϕ (deg.) =	*0.0*
Wall friction,	δ (deg.) =	*0.0*
Initial soil modulus,	E_i (kip/ft^2) =	*2500*
Poisson's ratio,	ν =	*0.25*
Soil unit weight,	γ_m (pcf) =	**141.9**
Adhesion factor,	α =	*1.00*
	Δ_{max}/H =	*0.02*

To show the sensitivity of the calculated force-deflection curve to variations in material parameters, force-deflection curves were plotted with altered inputs. Each input was altered individually, and then all high assumptions were combined for an overall high curve. All low assumptions were also combined for an overall low curve. Figure 3-43 shows the computed force-deflection curves along with the measured force-deflection curve. The figure also shows the portion of the computed curve influenced by different inputs. For example, soil modulus influences initial slope, but not peak force.

Note that an assumption of a more typical wall friction value of 70% of soil friction angle yields a result around 40% too low. This is further support for the idea that the wall friction angle must be higher than typically expected in order to explain the measured behavior.

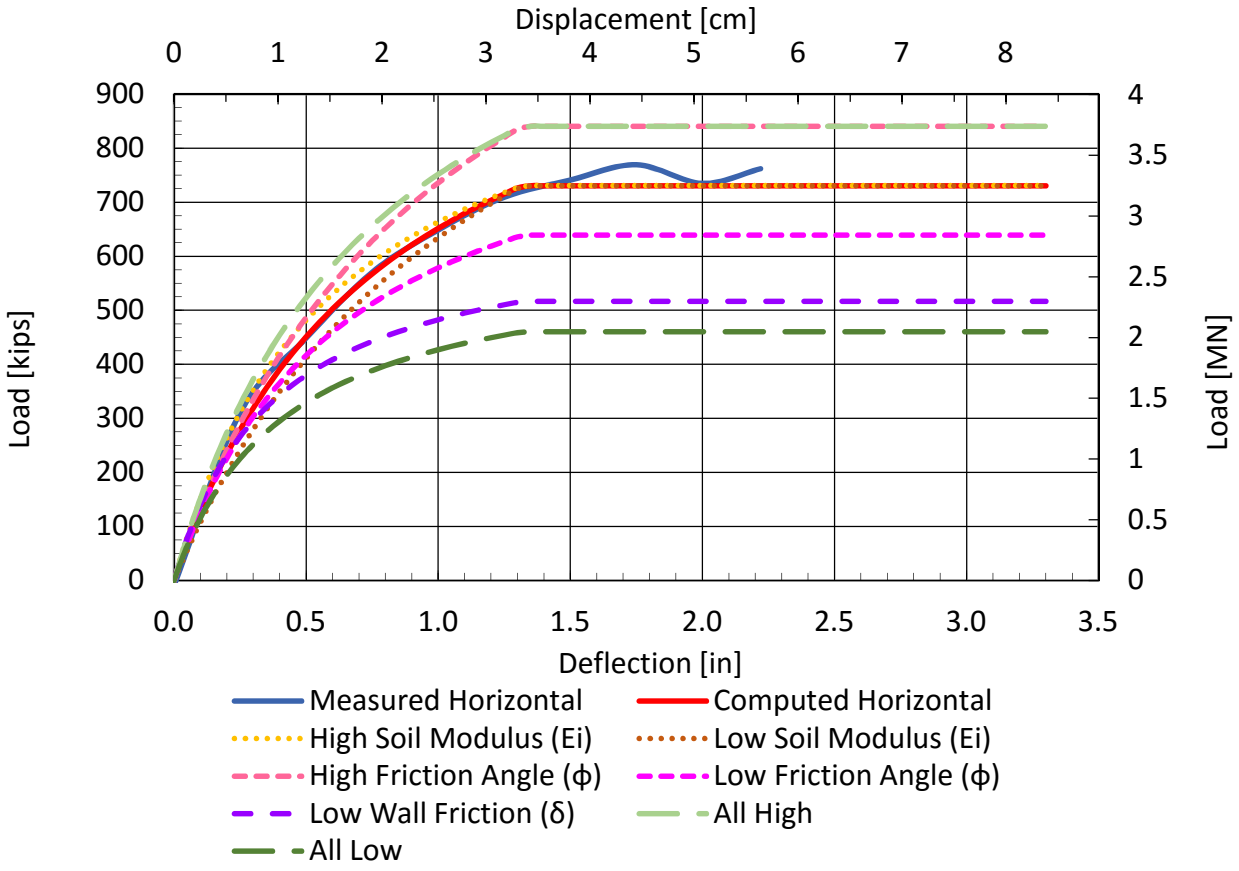

Figure 3-43. Measured and computed force-deflection curves for 0˚ skew assuming failure in the Type 2 (CTA) zone, using altered assumptions.

Table 3-5 gives the specific values used for each low, mid, and high parameter assumption. These values were arbitrarily chosen for the purpose of showing PYCAP sensitivity to differences in assumption values.

Table 3-5. Low, Mid and High Inputs for PYCAP Resulting in Computed Load-Deflection Curves

Input Description		Assumed Values		
		Low	Mid	High
Soil friction angle,	ϕ (deg.) =	45	46.0	47
Wall friction,	δ (deg.) =	0.7(ϕ)	1.0(ϕ)	1.0(ϕ)
Initial soil modulus,	E_i (kip/ft^2) =	2000	2500	3000

4 CONCLUSION

The research objectives for this thesis, as stated in Section 1.2, were to:

1. Determine passive force-displacement relationships for CTA transitional backfills from full-scale tests
2. Quantify the effect of skew angle on the passive force for CTA transitional backfills

The following sections will summarize the experimentation and the findings in relation to these objectives.

4.1 Summary

To investigate the passive force-displacement relationships provided by a transitional zoned backfill consisting of cement treated aggregate (CTA) with 3% cement and compacted gravel, a series of full-scale lateral abutment load tests were performed. The transitional zoned backfill was designed to minimize differential settlement adjacent to bridge abutments for the California High Speed Rail project. Tests were performed with a 2-D or plane strain backfill geometry to simulate a wide abutment; however, the abutment backwall was 5.5 ft. tall and 11 ft. wide. To investigate the effect of skew angle on the passive force, lateral abutment load tests were also performed on a simulated abutment with skew angles of 30º and 45º.

4.2 Findings

Based on the results of the field testing, the following conclusions have been developed relative to the transitional zoned backfill geometry proposed for California High Speed Rail:

1. The peak passive force developed was about 2.5 times higher than that predicted with the Caltrans design method for granular backfill material with a comparable backwall height and width.
2. The displacement required to develop the peak passive force decreased with skew angle and was somewhat less than for conventional granular backfills. Peak passive force developed with displacements of 1.8 to 3% of the wall height (H) in comparison to 3 to 5% of H for conventional granular backfills.
3. The skew angle had less effect on the peak passive force for the transitional backfill than for conventional granular backfills. For example, the passive force reduction factor, R_{skew}, was only 0.83 and 0.51 for the 30º and 45º skew abutments in comparison to 0.51 and 0.37 for conventional granular backfills.
4. Field measurements suggest that the CTA backfill largely moves with the abutment and does not experience significant heave while shear failure and heaving largely occurs in the granular backfill behind the CTA backfill zone.
5. Simplified passive force-deflection calculations can yield reasonable estimates of the measured curves by assuming that the CTA zone largely moves with the bridge abutment and causes passive shear failure in the gravel zone behind it. Therefore, passive force should be based on the friction angle of the gravel zone behind the CTA with a wall friction angle equal to that of the gravel zone. The conclusion presumes that the CTA and gravel backfill are compacted at the same time so that a rough cemented interface develops during curing of the CTA.

REFERENCES

Burke, M. P., Jr. (1994). “Semi-integral bridges: Movements and forces.” Transportation Research Record 1460, Transportation Research Board, Washington, DC, 1–7.

Cole, R. T. and Rollins, K. M. (2006) "Passive Earth Pressure Mobilization during Cyclic Loading." *Jounal of Geotechnical and Geoenvironmental Engineering,* 1154-1164.

Franke, B. W. (2013) "Passive Force on Skewed Abutments with Mechanically Stabilized Earth (MSE) Wingwalls Based on Large-Scale Tests." MS Thesis, Civil & Environmental Engineering, Brigham Young University, Provo, UT.

Fredrickson, A., Rollins, K.M., Nicks, J. (2017). Passive Force-Deflection Behavior of Geosynthetically Reinforced Soil (GRS) Backfill Based on Large-Scale Tests.” *Procs. Geotechnical Frontiers, Geotechnical Special Publication 278*, ASCE, p. 23-32.

Guthrie, W. S., Rogers, M. A. (2010). "Variability in Construction of Cement-Treated Base Layers." Transportation Research Record: Journal of the Transportation Research Board. Vol. 2186, p. 78-89.

Marsh, A., Rollins, K.M. (2013) "Behavior of Zero and Thirty Degree Skewed Abutments.” Journal of Transportation Research, Transportation Research Board, Washington, DC. Vol. 2363 (Soil Mechanics 2013), p. 12-20.

Nicks, J. E. (2009). "The Bump at the End of the Railway Bridge." Doctoral dissertation, Texas A&M University. Available electronically from http://hdl.handle.net/1969.1/ETD-TAMU-2009-12-7432.

Palmer, K. N. (2013). "Large-Scale Testing of Passive Force Behavior for Skewed Abutments with High Width-Height Ratios." M.S. Thesis, Civil & Environmental Engineering, Brigham Young University, Provo, Utah.

Paixão, A., et al. (2013). "Design and Construction of Backfills for Railway Track Transition Zones." *Proceedings of the Institution of Mechanical Engineers, Part F: Journal of Rail and Rapid Transit:* 58-70.

Rollins, K. M. and Jessee, S. (2013). "Passive Force-Deflection Curves for Skewed Abutments." *J. Bridge Engineering*, ASCE, Vol. 18, No. 10, p. 1086-1094

Rollins, K. M. and Sparks, A. (2002) "Lateral Resistance of Full-Scale Pile Cap with Gravel Backfill." *J. Geotechnical and Geoenviron. Engrg.,* ASCE, Vol. 128 No. 9 711-723.

Rollins, K.M. and Cole, R.T. (2006). "Cyclic Lateral Load Behavior of a Pile Cap and Backfill." *J. Geotechnical and Geoenviron. Engrg*., ASCE, Vol. 132, No. 9, 1143-1153.

Shamsabadi, A. and Rollins, K.M. (2014). "Three-dimensional nonlinear continuum seismic soil-structure interaction analysis of skewed bridge abutments." *Procs., Eighth European Conference on Numerical Methods in Geotechnical Engineering*, Delft, the Netherlands, 6 p.

Shamsabadi, A., Rollins, K.M., Kapaskur, M. (2007). “Nonlinear Soil-Abutment-Bridge Structure Interaction for Seismic Performance-Based Design.” *J. Geotechnical Geoenviron. Engrg.*, ASCE, Vol. 133, No. 6, 707-720.

Shamsabadi, A., S. Xu, and E. Taciroglu. (2013) *Development of Improved Guidelines for Analysis and Design of Earth Retaining Structures. Report CA13-2270*. Los Angeles, CA: Department of Civil and Environmental Engineering, University of California, Los Angeles, July 2013.

Smith, J. C. (2014). "Evaluation of Passive Force Behavior for Bridge Abutments Using Large-Scale Tests with Various Backfill Geometries." M.S. Thesis, Civil & Environmental Engineering, Brigham Young University, Provo, Utah.

Soil-Cement Laboratory Handbook. (1992) Publication EB052.07S. Portland Cement Association, Skokie, IL.

Wagstaff, K. B., (2016). "Evaluation of Passive Force on Skewed Bridge Abutments with Controlled Low-Strength Material Backfill." M.S. Thesis, Civil & Environmental. Engineering, Brigham Young University, Provo, Utah.